

Active Zone Proteins RIM1 $\alpha\beta$ Are Required for Normal Corticostriatal Transmission and Action Control

David A. Kupferschmidt,^{1,2} Shana M. Augustin,¹ Kari A. Johnson,¹ and David M. Lovinger¹

¹Section on Synaptic Pharmacology & In Vivo Neural Function, Laboratory for Integrative Neuroscience, National Institute on Alcohol Abuse and Alcoholism, National Institutes of Health, Rockville, Maryland 20852, and ²Integrative Neuroscience Section, National Institute of Neurological Disorders and Stroke, National Institutes of Health, Bethesda, Maryland 20892

Dynamic regulation of synaptic transmission at cortical inputs to the dorsal striatum is considered critical for flexible and efficient action learning and control. Presynaptic mechanisms governing the properties and plasticity of glutamate release from these inputs are not fully understood, and the corticostriatal synaptic processes that support normal action learning and control remain unclear. Here we show in male and female mice that conditional deletion of presynaptic proteins RIM1 $\alpha\beta$ (RIM1) from excitatory cortical neurons impairs corticostriatal synaptic transmission in the dorsolateral striatum. Key forms of presynaptic G-protein-coupled receptor-mediated short- and long-term striatal plasticity are spared following RIM1 deletion. Conditional RIM1 KO mice show heightened novelty-induced locomotion and impaired motor learning on the accelerating rotarod. They further show heightened self-paced instrumental responding for food and impaired learning of a habitual instrumental response strategy. Together, these findings reveal a selective role for presynaptic RIM1 in neurotransmitter release at prominent basal ganglia synapses, and provide evidence that RIM1-dependent processes help to promote the refinement of skilled actions, constrain goal-directed behaviors, and support the learning and use of habits.

Key words: action; corticostriatal; learning; plasticity; RIM1; transmission

Significance Statement

Our daily functioning hinges on the ability to flexibly and efficiently learn and control our actions. How the brain encodes these capacities is unclear. Here we identified a selective role for presynaptic proteins RIM1 $\alpha\beta$ in controlling glutamate release from cortical inputs to the dorsolateral striatum, a brain structure critical for action learning and control. Behavioral analysis of mice with restricted genetic deletion of RIM1 $\alpha\beta$ further revealed roles for RIM1 $\alpha\beta$ -dependent processes in the learning and refinement of motor skills and the balanced expression of goal-directed and habitual actions.

Introduction

The capacities to select, refine, and automatize actions arise from concerted activity and plasticity of multiple, interconnected neural networks. Central to these networks is the dorsal striatum, the primary input nucleus of the basal ganglia (Balleine et al., 2007; Heilbronner et al., 2016). Excitatory projections emanating

broadly from cerebral cortex, thalamus, and amygdala innervate the dorsal striatum in complex patterns (Kelley et al., 1982; McGeorge and Faull, 1989; Smith et al., 2004; Hintiryan et al., 2016; Hunnicutt et al., 2016), contributing to functional heterogeneity across its various subregions. For example, the learning and use of goal-directed action strategies preferentially recruit and rely on dorsomedial striatal subregions (Barnes et al., 2005; Yin et al., 2005a,b; Thorn et al., 2010; Corbit et al., 2013; Gremel and Costa, 2013; Hart et al., 2018), whereas habitual strategies and skilled action patterns preferentially engage and depend on intact dorsolateral subregions (Yin et al., 2004, 2006, 2009; Dias-Ferreira et al., 2009; Thorn et al., 2010; Kupferschmidt et al., 2017). By gating and integrating diverse inputs across these subregions, the dorsal striatum functions to facilitate adaptive behavioral control (Graybiel and Grafton, 2015; Rueda-Orozco and Robbe, 2015; Peak et al., 2018).

Cortical inputs provide a primary source of excitatory drive of dorsal striatal neurons (Wilson, 1995; Huerta-Ocampo et al.,

Received July 26, 2018; revised Nov. 13, 2018; accepted Dec. 4, 2018.

Author contributions: S.M.A., K.A.J., and D.M.L. edited the paper. D.A.K. and D.M.L. designed research; D.A.K., S.M.A., and K.A.J. performed research; D.A.K. and K.A.J. analyzed data; D.A.K. wrote the paper.

This work was supported by National Institute on Alcohol Abuse and Alcoholism Division of Intramural Clinical and Biological Research ZIA AA000416, National Sciences and Engineering Research Council postdoctoral fellowship 438487-13 to D.A.K., and National Institute of General Medical Sciences PRAT Fellowship and K99 AA025403 to K.A.J. We thank all members of the D.M.L. laboratory for helpful discussions about the present experiments and manuscript; Guoxiang Luo for help with mouse genotyping; and the Fishers Lane Animal Care staff for excellent animal husbandry.

The authors declare no competing financial interests.

Correspondence should be addressed to David M. Lovinger at lovindav@mail.nih.gov.

<https://doi.org/10.1523/JNEUROSCI.1940-18.2018>

Copyright © 2019 the authors 0270-6474/19/391457-14\$15.00/0

2014); thus, dynamic changes in corticostriatal transmission are considered key determinants of dorsal striatum function and adaptive actions. Postsynaptic plasticity at putative corticostriatal synapses has been well established to contribute to action learning and control (Costa et al., 2004; Barnes et al., 2005; Yin et al., 2005a, 2006, 2009; Dang et al., 2006; Pittenger et al., 2006; Hawes et al., 2015; Santos et al., 2015). Glutamate release from corticostriatal terminals is also potently modulated by various presynaptic signaling and plasticity processes (Calabresi et al., 1990; Lovinger, 1991; Atwood et al., 2014; Park et al., 2014; Kupferschmidt and Lovinger, 2015). *Ex vivo* electrophysiology and gene deletion studies suggest roles for presynaptic plasticity at corticostriatal terminals in skill learning (Barnes et al., 2005; Kheirbek et al., 2009; Yin et al., 2009; Hawes et al., 2015), and manipulations of presynaptic corticostriatal receptor function bias the learning and use of goal-directed and habitual action strategies (Nazzaro et al., 2012; Gremel et al., 2016). Notably, loss of presynaptic cannabinoid-1 receptor (CB1R)-dependent long-term depression (LTD) of excitatory transmission in the dorsolateral striatum (DLS) has been proposed to promote habit formation (Nazzaro et al., 2012), whereas endocannabinoid signaling in dorsomedial striatum fosters habit formation (Gremel et al., 2016). Furthermore, *in vivo* monitoring of corticostriatal input function has revealed presynaptic activity dynamics that encode and predict action learning (Kupferschmidt et al., 2017). Despite these advances, little is known about the synaptic mechanisms through which corticostriatal transmission supports action learning and control.

Rab3-interacting molecules (RIMs) are presynaptic scaffold proteins that coordinate key active zone processes involved in synaptic transmission (Südhof, 2013). RIMs form the core of a macromolecular complex that recruits voltage-gated calcium channels to active zones, docks synaptic vesicles to the exocytotic machinery, and primes them for release (Wang et al., 1997; Coppola et al., 2001; Hibino et al., 2002; Sun et al., 2003; Deng et al., 2011; Han et al., 2011; Kaeser et al., 2011). Seven different RIM isoforms are encoded by four genes (*Rims1–4*), the first of which gives rise to isoforms RIM1 α and RIM1 β (collectively, RIM1) (Kaeser et al., 2008a). These isoforms are expressed widely in brain, with particularly high mRNA and protein levels in forebrain and cerebellar structures (Schoch et al., 2006; Kaeser et al., 2008a). Global and conditional knockout (KO) of RIM1 isoforms has revealed synapse-specific roles for the proteins in synaptic transmission and presynaptically expressed plasticity (Castillo et al., 2002; Schoch et al., 2002; Calakos et al., 2004; Chevalyere et al., 2007; Fourcaudot et al., 2008; Kaeser et al., 2008b; Grueter et al., 2010). For example, RIM1 α deletion selectively impairs synaptic transmission and short-term plasticity at hippocampal Schaffer collateral-CA1 synapses (Schoch et al., 2002), whereas mossy fiber synapses show selective deficits in long-term plasticity after such deletion (Castillo et al., 2002; Yang and Calakos, 2010). These and other synaptic phenotypes have been linked to behavioral abnormalities following RIM1 deletion, including altered maternal behavior, fear and spatial learning, locomotion, and prepulse inhibition (Schoch et al., 2002; Powell et al., 2004; Blundell et al., 2010; Haws et al., 2012). Despite the importance of corticostriatal transmission and its presynaptic regulation to dorsal striatal function, the contributions of RIM1 to these synaptic processes have yet to be tested. Moreover, the discrete presynaptic proteins and processes within corticostriatal inputs that support action learning and control remain poorly understood.

Here we show that conditional deletion of RIM1 from cortical pyramidal neurons, including corticostriatal projection neurons,

impairs excitatory transmission in the DLS, but spares forms of GPCR-mediated short- and long-term striatal plasticity. Conditional RIM1 KO mice show heightened novelty-induced locomotion and impaired motor learning on the accelerating rotarod. They further show heightened instrumental responding for food under higher-effort conditions and impaired expression of habitual food responding. These findings implicate RIM1-dependent processes in corticostriatal transmission and in the learning and control of motivated behavior.

Materials and Methods

Mice

All mice used in these experiments were obtained from The Jackson Laboratory and backcrossed onto a C57BL/6J background (stock #000664) for at least 5 generations. Floxed RIM1 mice (*RIM1^{fl/fl}*, stock #015832) (Kaeser et al., 2008a) that carry loxP sites flanking exon 6 of the *RIM1* gene were bred with *Emx1::Cre* mice (stock #005628) (Gorski et al., 2002) that express Cre recombinase in the majority of excitatory cells in the neocortex and hippocampus (and sparser populations in some ventral pallial structures) using a 3-stage breeding strategy: (1) *Emx1::Cre* mice were crossed with *RIM1^{fl/fl}* mice; (2) *Emx1::Cre;RIM1^{+/+}* offspring were crossed with *RIM1^{fl/fl}* mice; and (3) *Emx1::Cre;RIM1^{-/-}* offspring were crossed again with *RIM1^{fl/fl}* mice. This strategy generated age- and sex-matched littermates with RIM1 either present in (*RIM1^{fl/fl}*; Control) or deleted from *Emx1^{Cre}*-expressing cells (*Emx1::Cre;RIM1^{-/-}*). Mice were housed in groups of 2–4 in a humidity- and temperature-controlled colony room on a 12 h light/dark cycle with *ad libitum* access to water and food (unless otherwise specified). Mice that underwent testing for novelty-induced locomotion were later tested for motor learning on the accelerating rotarod and prepulse inhibition. Mice tested for homecage locomotion, fixed ratio (FR)/progressive ratio (PR) instrumental training, and fixed/random interval (RI) instrumental training comprised 3 separate cohorts. All procedures conformed to the National Institutes of Health *Guide to the care and use of laboratory animals* and were approved by the National Institute on Alcohol Abuse and Alcoholism Animal Care and Use Committee.

qRT-PCR

Mice were anesthetized with isoflurane and decapitated, and brains were rapidly removed and rinsed in cold 0.9% NaCl. Brains were cut into 1 mm coronal sections using a stainless-steel brain matrix, and samples from M1+M2 motor cortices, dorsal striatum, or thalamus were placed in RNAlater (Invitrogen), stored at 4°C for 48 h, then removed from RNAlater and frozen at –20°C before RNA extraction. RNA was extracted using the RNeasy Lipid Tissue Mini Kit (QIAGEN), and RNA concentration was measured using a NanoDrop (Thermo Fisher Scientific). RNA (100 ng) was reverse transcribed using the Quantitect Reverse Transcription Kit (QIAGEN). qPCRs contained 2 μ l cDNA template, 1 μ l predesigned TaqMan Gene Expression Assay (for *Rim1*, Mm01225745_m1), 10 μ l TaqMan Fast Advanced Master Mix (both from Thermo Fisher Scientific), and 7 μ l Ultrapure water (Invitrogen). qPCR was run on StepOnePlus system (Thermo Fisher Scientific) and was performed according to the manufacturer's recommended settings: 50°C for 2 min, 95°C for 2 min, and then 40 cycles of melting at 95°C for 1 s and annealing/extension at 60°C for 20 s. Reactions were run in triplicate for 4 or 5 animals per group. Analysis was performed using the $2^{-\Delta C_T}$ method (Schmittgen and Livak, 2008). The C_T value was determined by identifying the cycle number at which the amplification curve reached a ΔR_n threshold set at 0.1 ($\Delta R_n = R_n - \text{baseline}$, where R_n is the fluorescence of the reporter dye divided by the fluorescence of a passive reference dye). Relative *Rim1* mRNA expression was quantified using *Actb* as an internal control (Applied Biosystems #4351315). Thus, $\Delta C_T = C_T(\text{Rim1}) - C_T(\text{Actb})$.

Immunohistochemistry

RIM1^{fl/fl} and *Emx1::Cre;RIM1^{-/-}* mice were transcardially perfused under deep isoflurane anesthesia with 0.1 M PBS and 4% formaldehyde in PBS, pH 7.4. Brains were collected and postfixed in 4% formaldehyde at

4°C for 24 h. The 50 μ m coronal sections were made using a vibratome. On a revolving platform, sections were incubated in PBST (PBS with 0.2% Triton X-100) for 2 h, and blocked in 5% BSA in PBST for 4 h. Slices were then incubated in chicken anti-Neurofilament (Encor Biotechnology, catalog #CPCA-NF-H, 1:40,000) with rabbit anti-mu opioid receptor (Immunostar, 24216, 1:4000), rabbit anti-parvalbumin (Swant, PV27, 1:1000), or rabbit anti-cannabinoid-1 receptor (CB1R; Synaptic Systems, 258003, 1:1000) antibodies in PBST for 12 h at 4°C. Following three 1 h washes in PBST, slices were incubated in AlexaFluor-488 goat anti-chicken (Invitrogen, A-11039, 1:2000), AlexaFluor-488 goat anti-rabbit (Invitrogen, A-11034, 1:1000), and/or AlexaFluor-568 goat anti-rabbit (Invitrogen, A-11011, 1:1000) antibodies in PBST for 12 h at 4°C. Following a 1 h wash in PBST containing DAPI (Invitrogen, D3571, 1:20,000) and three 1 h washes in PBS, sections were mounted on Superfrost Plus slides (Daigger, EF15978Z) using Fluoromount Aqueous Mounting Medium (Sigma-Aldrich, F4680), coverslipped, and imaged using Carl Zeiss AxioVision LE 4.3 software with a Carl Zeiss AxioCam on a Carl Zeiss Stereo Lumar microscope. Brightness was uniformly adjusted in each image for presentation.

Electrophysiology

Brain slice preparation for electrophysiology. Following isoflurane anesthesia, $RIM1^{fl/fl}$ and $Emx1::Cre;RIM1^{-/-}$ mice (P18–P50) were decapitated, and brains were rapidly removed and submerged in ice-cold cutting solution containing the following (in mM): 30 NaCl, 4.5 KCl, 1 $MgCl_2$, 26 $NaHCO_3$, 1.2 NaH_2PO_4 , 10 glucose, and 194 sucrose, continuously bubbled with 95% O_2 /5% CO_2 . Slices were submerged in aCSF containing the following (in mM): 124 NaCl, 4.5 KCl, 2 $CaCl_2$, 1 $MgCl_2$, 26 $NaHCO_3$, 1.2 NaH_2PO_4 , and 10 glucose, in a holding chamber and continuously bubbled with 95% O_2 /5% CO_2 . Slices were incubated for 30 min at 32°C and then held at room temperature for 1–5 h before whole-cell recordings.

Whole-cell voltage-clamp recordings (excluding depolarization-induced suppression of excitation [DSE] and DHPG experiments). Individual hemisected slices were moved to a custom recording chamber where they were submerged in and continuously perfused with 30°C–32°C aCSF containing picrotoxin (50 μ M) at a rate of \sim 1.5 ml/min. Borosilicate glass pipettes (2.5–4.0 M Ω resistance in bath) were filled with internal solution (295–310 mOsm, pH 7.3) containing the following (in mM): 120 CsMeSO₃, 5 NaCl, 10 tetraethylammonium-Cl, 10 HEPES, 5 QX-314, 1.1 EGTA, 0.3 Na-GTP, and 4 Mg-ATP. Slices were visualized on a Olympus BX51WI microscope with a 40 \times /0.8 NA water-immersion objective. EPSCs were recorded from medium-sized spiny projection neurons (MSNs) held at -60 mV using a Multiclamp 700A amplifier and Digidata 1332A (Molecular Devices). Recordings were filtered at 2 kHz and digitized at 10 kHz using Clampex 10.3 software (Molecular Devices). A concentric bipolar stimulating electrode (FHC, CBAEC75), controlled by an isolation unit (Digitimer, DS3) and Clampex 10.3, was placed at the border of the DLS and the overlying white matter. Electrical pulses were delivered every 20 s. Stimulation duration (40–80 μ s) and intensity (40–100 μ A) were adjusted to yield EPSC amplitudes of 200–500 pA. Experiments were discarded if series resistance varied by $>20\%$ or increased >25 M Ω . Data were analyzed using Clampfit 10.3.

Whole-cell voltage-clamp recordings (DSE experiments). Recordings were performed as described above, with the following exceptions. Recording pipettes were filled with a potassium-based internal solution containing the following (in mM): 120 K-gluconate, 4 NaCl, 20 KCl, 10 HEPES, 0.4 Na-GTP, and 4 Mg-ATP, pH adjusted to 7.25 using KOH. Neurons were held at -70 mV, and electrical pulses were delivered every 5 s. EPSC amplitudes were monitored for 50 s before and 100 s after DSE induction. DSE was induced by depolarizing the neuron to 30 mV for 10 s. The data were averaged from 3 trials per cell. For each trial, EPSC amplitudes were normalized to the average baseline amplitude, and between-group comparisons were made on the first EPSC following DSE induction.

Whole-cell voltage-clamp recordings (DHPG experiments). EPSCs were recorded through pipettes of 3–5 M Ω in MSNs held at -50 mV. EPSCs were evoked every 20 s by a tungsten bipolar stimulating electrode (FHC) with a tip separation of 505 μ m placed in the DLS near the border of the

external capsule adjacent to the recorded neuron. Stimulation intensity was adjusted to yield EPSC amplitudes of 200–400 pA. Experiments were discarded if series resistance varied by $>15\%$ or increased >20 M Ω .

Homecage locomotion

$RIM1^{fl/fl}$ and $Emx1::Cre;RIM1^{-/-}$ mice were individually housed in standard homecages. Mice were then habituated to the locomotor testing room for 1 h/d for 3 d immediately following onset of the dark cycle. On the fourth day, mice were moved to the locomotor testing room for 1 h and then placed into a clean homecage. Horizontal activity was monitored using a photobeam-based system (San Diego Instruments) for 72 consecutive hours, across normal light-dark cycles.

Novel cage locomotion

$RIM1^{fl/fl}$ and $Emx1::Cre;RIM1^{-/-}$ mice were habituated to the locomotor testing room for 1 h/d for 3 d 1–2 h following onset of the light cycle. On the fourth day, mice were individually placed in clear Plexiglas rectangular chambers with minimal bedding, and horizontal activity was monitored using the photobeam-based tracking system for 2 h/d for 6 d. For one cohort of mice, used chambers were exchanged daily with clean chambers (“novel” cage each day); for another cohort, chambers remained unchanged across the 6 d of locomotor testing.

Prepulse inhibition

Prepulse inhibition was assessed in $RIM1^{fl/fl}$ and $Emx1::Cre;RIM1^{-/-}$ mice using procedures similar to those used previously (Blundell et al., 2010) in $RIM1\alpha$ KO mice. A startle chamber (San Diego Instruments) was fixed above a piezoelectric accelerometer and enclosed in a sound-attenuating box (Med Associates). Acoustic stimuli were delivered by a speaker mounted inside the box, 20 cm above the startle chamber. Chamber sensitivity and sound levels were calibrated before the experiment. Each startle response was recorded over a 65 ms period and quantified in arbitrary units. Mice underwent 62 trials of five trial types across a 22 min session: pulse alone (40 ms pulse of 120 dB white noise), three different prepulse/pulse trials (20 ms prepulse of 4, 8, or 16 dB above background noise level of 70 dB preceding 100 ms, 120 dB pulse; onset to onset), and no stimulus. Trials were presented pseudo-randomly with an average intertrial interval of 15 s (7–23 s). A 5 min acclimation period preceded testing in four blocks of trials. Blocks 1 and 4 consisted of six pulse-alone trials; blocks 2 and 3 contained six pulse-alone trials, five of each level of prepulse/pulse, and five no-stimulus trials. Prepulse inhibition was assessed as the percentage of decrease in startle amplitude in prepulse/pulse trials compared with pulse-alone trials.

Accelerating rotarod

$RIM1^{fl/fl}$ and $Emx1::Cre;RIM1^{-/-}$ mice were trained on a rotarod (ENV-575M, Med Associates) that accelerated from 4 to 40 rpm over 300 s. Latency to fall from the rotarod was recorded during 4 trials per day for 3 d, with 15 min between trials. Individual trials were stopped and latency was recorded if the mouse held onto the rod for two consecutive rotations or reached 40 rpm.

Self-paced instrumental training

Eight identical operant chambers (Med Associates) enclosed in sound- and light-attenuating cases were used for instrumental training. Each chamber was equipped with a pellet dispenser that delivered food pellets (F0071, Bioserv) into a recessed food magazine, an infrared photobeam crossing the magazine to allow detection of magazine head entries, two retractable levers to either side of the magazine, a houselight, and a steel rod floor. A computer running Med-PC software (Med Associates) controlled operant chamber events and recorded lever presses and magazine entries.

$RIM1^{fl/fl}$ and $Emx1::Cre;RIM1^{-/-}$ mice were food restricted to 90%–95% of their free-feeding body weight, and handled daily for 2 d before training on one of two instrumental paradigms: [1] FR training and PR testing, and [2] RI training and valuation testing.

FR training and PR testing

Following 2 d of food restriction and handling, $RIM1^{fl/fl}$ and $Emx1::Cre;RIM1^{-/-}$ mice were given one 15 min session of magazine training,

during which food pellets were delivered at random 60 s intervals for 15 outcomes. Mice were then trained to press one of two available levers for food pellets in daily 90 min sessions. Responses on the “active” lever resulted in pellet delivery, whereas responses on the “inactive” lever did not. Mice were trained on an FR1 schedule for 5 d with the potential to earn up to 10 and 20 rewards on training days 1 and 2, respectively, and 30 rewards on days 3–5. Mice were then trained on an FR5 schedule for 2 d, and an FR10 schedule for 2 d, each with the potential to earn 30 rewards/d. Mice were then tested in one session on a PR schedule wherein mice had to press the active lever a progressively increasing number of times (10, 20, 25, 32, 40, 50, etc.) (adapted from Richardson and Roberts, 1996) to obtain successive food pellets. The total number of lever presses and the breakpoint achieved (defined as the last series in which a pellet was obtained) were recorded.

RI training and valuation testing

A separate cohort of $RIM1^{fl/fl}$ and $Emx1::Cre;RIM1^{-/-}$ mice were food restricted to 90%–95% of their baseline body weight. Following 2 d of food restriction and handling, mice were given one 15 min session of magazine training, during which food pellets were delivered at random 60 s intervals for 15 outcomes. Mice were then trained to press a single lever for food pellets in daily 90 min sessions on FR1 for 4–5 d, RI30 for 2 d, and RI60 for 4 d. One to 3 h following each training session, mice were given 1 h access to a 20% sucrose solution in their homecages.

Valuation testing was conducted on the 2 d following training. On the valued day, mice were given *ad libitum* access to the sucrose solution for 1 h before a 5 min unreinforced session in the operant boxes. On the devalued day, mice were given *ad libitum* access to the food pellets previously earned by lever pressing for 1 h before a 5 min unreinforced session in the operant boxes.

Drugs

Picrotoxin (Sigma-Aldrich) was dissolved directly in aCSF. LY379268 and (RS)-3,5-DHPG (Tocris Bioscience) were prepared in distilled H₂O and aCSF, respectively, and diluted to their final concentrations in aCSF. AM251 (Tocris Bioscience) was prepared in DMSO (Sigma-Aldrich) and diluted to its final concentration in aCSF containing β -cyclodextrin (6% w/v; TCI America) as a carrier. The final concentration of DMSO was <0.1%.

Statistics

Data are mean \pm SEM. One-sample Student's *t* tests were used to compare a single genotype ($RIM1^{fl/fl}$ or $Emx1::Cre;RIM1^{-/-}$) to a theoretical mean (e.g., 100% EPSC amplitude baseline). Two-tailed paired or unpaired Student's *t* tests were used to compare $RIM1^{fl/fl}$ or $Emx1::Cre;RIM1^{-/-}$ mice on a single measure (e.g., sEPSC frequency). A nonparametric Mann–Whitney test was used to compare $RIM1^{fl/fl}$ or $Emx1::Cre;RIM1^{-/-}$ mice breakpoints in PR schedule responding. Two-way mixed ANOVAs were used to assess main effects and interactions of genotype with repeated-measures variables (e.g., paired pulse ratios at multiple interpulse intervals in $RIM1^{fl/fl}$ or $Emx1::Cre;RIM1^{-/-}$ mice). *Post hoc* significance was determined using Sidak's multiple-comparisons test. A hierarchical linear mixed model was used to assess main effects and interactions of genotype with repeated-measures variables that contain nested variables (e.g., rotarod latencies across trials nested within days in $RIM1^{fl/fl}$ and $Emx1::Cre;RIM1^{-/-}$ mice). All pair-

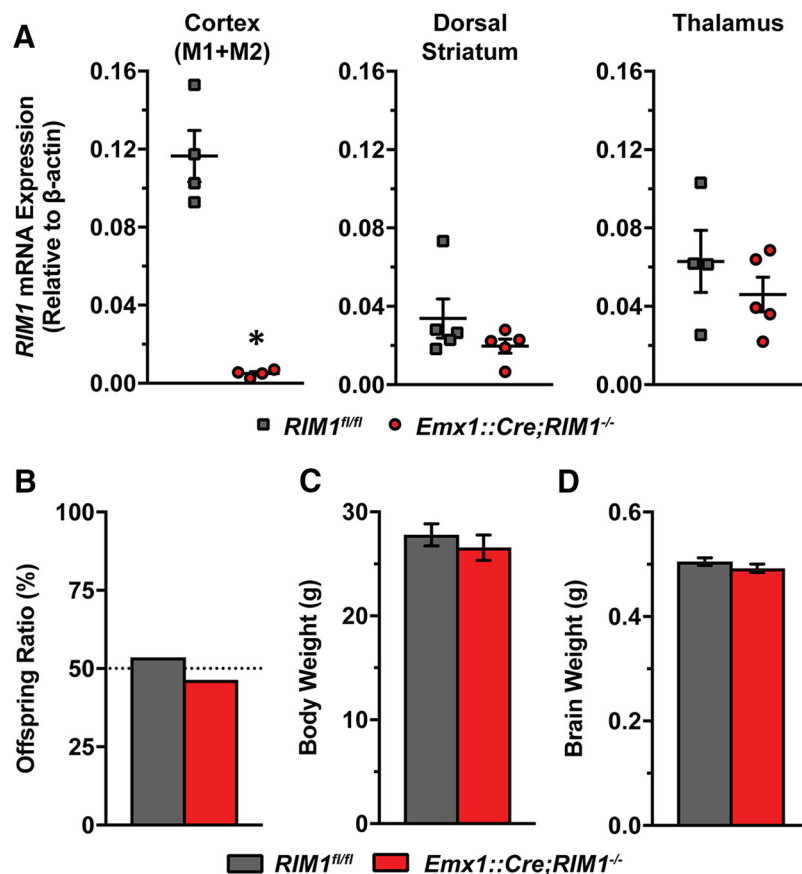


Figure 1. Conditional RIM1 KO reduced cortical gene expression and was without effect on viability, body weight, and brain weight. **A**, qRT-PCR measurement of RIM1 mRNA in cortex, dorsal striatum, and thalamus of $RIM1^{fl/fl}$ and $Emx1::Cre;RIM1^{-/-}$ mice. * $p < 0.05$, different from $RIM1^{fl/fl}$ group. **B**, Offspring ratios of $RIM1^{fl/fl}$ and $Emx1::Cre;RIM1^{-/-}$ mice. **C**, Average body weights of adult (P90–P100) $RIM1^{fl/fl}$ and $Emx1::Cre;RIM1^{-/-}$ mice. **D**, Average brain weights of adult (P90–P100) $RIM1^{fl/fl}$ and $Emx1::Cre;RIM1^{-/-}$ mice.

wise comparisons of the model-derived estimated marginal means underwent Bonferroni corrections, and all reported *p* values reflect these corrections. Sex differences were analyzed for each category of behavior using one-sample Student's *t* tests and two-way ANOVAs, where appropriate. Effects were considered statistically significant at $p < 0.05$. Data were analyzed using MiniAnalysis, Clampfit, Microsoft Excel, GraphPad Prism 6, and PASW Statistics 18.

Results

Verification of conditional RIM1 KO

To assess the efficacy of our conditional RIM1 deletion strategy, we performed qRT-PCR on brain samples from $RIM1^{fl/fl}$ and $Emx1::Cre;RIM1^{-/-}$ mice. Consistent with the known expression patterns of $Emx1::Cre$ mice (Gorski et al., 2002), RIM1 mRNA was reduced in motor cortex (M1 and M2) of $Emx1::Cre;RIM1^{-/-}$ mice relative to $RIM1^{fl/fl}$ littermates (Fig. 1A; $n = 4$, $n = 4$; $t_{(6)} = 8.421$, $p < 0.0005$) but was indistinguishable from controls in dorsal striatum ($n = 5$, $n = 5$; $t_{(8)} = 1.327$, $p = 0.221$) and thalamus ($n = 4$, $n = 5$; $t_{(7)} = 0.986$, $p = 0.357$).

Normal viability, brain and body weight, and gross brain morphology in conditional RIM1 KO mice

$Emx1::Cre;RIM1^{-/-}$ mice were viable and fertile. Offspring of $Emx1::Cre;RIM1^{-/-} \times RIM1^{fl/fl}$ were born at the expected Mendelian ratios (Fig. 1B), and survived normally into adulthood. Body and brain weights of $Emx1::Cre;RIM1^{-/-}$ mice did not

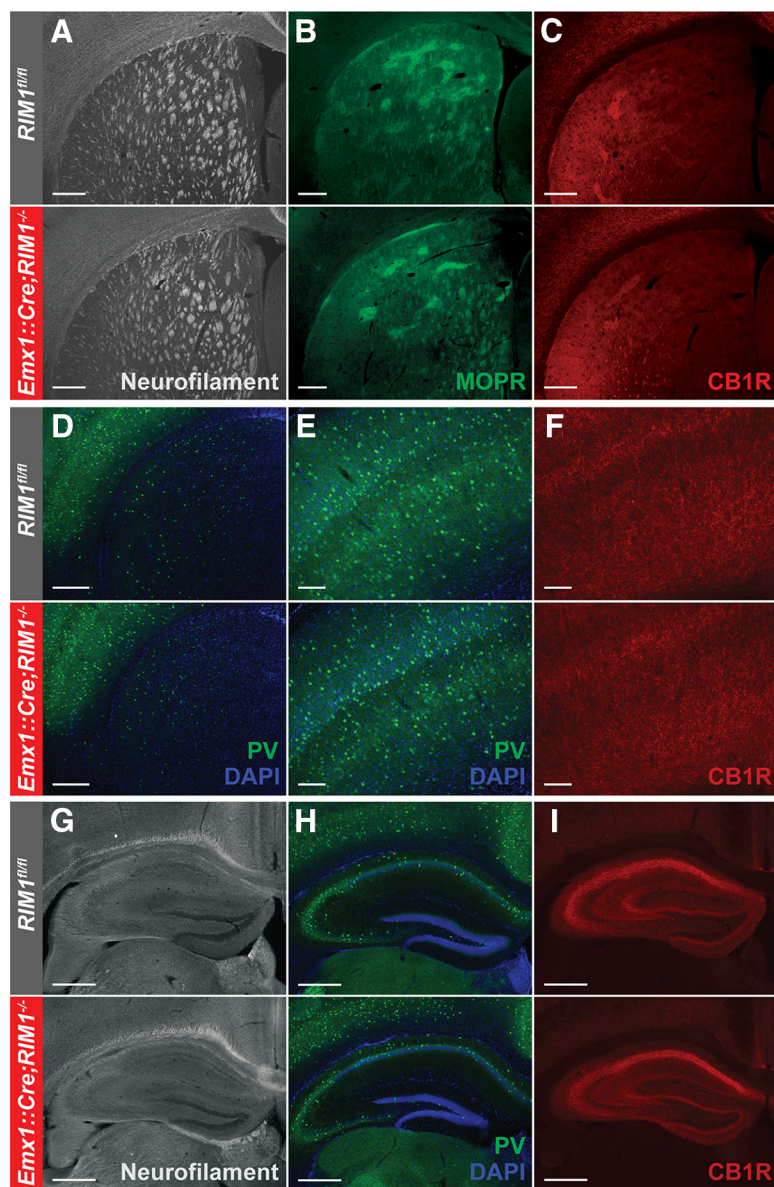


Figure 2. Gross brain anatomy is unaltered in conditional RIM1 KO mice. **A–I**, Neurofilament, CB1R, mu opioid receptor (MOPR), parvalbumin (PV), and/or DAPI staining of striatum (**A–D**), motor cortex (**E,F**) and hippocampus (**G–I**) of $RIM1^{fl/fl}$ and $Emx1::Cre;RIM1^{fl/fl}$ mice. Scale bars: **A–D, G–I**, 400 μ m; **E, F**, 200 μ m.

differ from those of littermate $RIM1^{fl/fl}$ controls (Fig. 1C: $n = 14$, $n = 16$; $t_{(28)} = 0.766$, $p = 0.45$; Fig. 1D: $n = 7$, $n = 8$; $t_{(13)} = 1.17$, $p = 0.263$). Morphological analyses revealed no gross structural abnormalities in brain architecture in the conditional RIM1 KO mice. Notably, unlike mice with *Emx1* promoter-driven conditional KO of the presynaptic CB1R (Davis et al., 2018), $Emx1::Cre;RIM1^{fl/fl}$ mice showed normal axonal fasciculation of cortical fibers into and through striatum as revealed by immunostaining for neurofilament (Fig. 2A). Striatal CB1R and mu opioid receptor expression patterns were also normal in $Emx1::Cre;RIM1^{fl/fl}$ mice (Fig. 2B,C), indicating preserved striosome-matrix striatal compartments in mice lacking cortical RIM1. Mesoscale cortical and hippocampal structure was similarly preserved in these mice, as indicated by labeling with DAPI and immunostaining for neurofilament, parvalbumin, and CB1R (Fig. 2D–I).

Impaired excitatory transmission at corticostriatal synapses in conditional RIM1 KO mice

Given our interest in probing the role of corticostriatal RIM1 in action learning and control, we examined synaptic transmission and plasticity in the conditional RIM1 KO mice at cortical inputs to the DLS, a brain region widely implicated in the development and expression of habitual behaviors (Yin et al., 2004; Balleine et al., 2007). Furthermore, despite evidence of diverse, synapse-specific roles for RIM1 α in transmission and plasticity at several central projections (Castillo et al., 2002; Schoch et al., 2002; Chevaleyre et al., 2007; Kiyonaka et al., 2007; Fourcaudot et al., 2008; Kintscher et al., 2013), and detailed characterization of presynaptic forms of plasticity at cortical inputs to the DLS (Gerdeman et al., 2002; Mathur et al., 2011; Atwood et al., 2014), no studies to date have determined physiological roles for RIM1 at corticostriatal synapses in the DLS, or dorsal striatum more generally.

To assess the contribution of RIM1 to excitatory transmission in the DLS, we first examined spontaneous excitatory postsynaptic current (sEPSC) frequency, amplitude, and kinetics in DLS MSNs of $Emx1::Cre;RIM1^{fl/fl}$ and $RIM1^{fl/fl}$ mice. sEPSC frequency was significantly reduced in $Emx1::Cre;RIM1^{fl/fl}$ relative to $RIM1^{fl/fl}$ mice (Fig. 3A; $n = 15$, $n = 15$, $t_{(28)} = 2.207$, $p < 0.05$). However, conditional deletion of RIM1 had no effect on sEPSC amplitude (Fig. 3B; $t_{(28)} = 1.624$, $p = 0.116$). sEPSC rise time, decay time, and total charge transfer were indistinguishable between the two groups (data not shown). These findings suggest that loss of RIM1 in cortical excitatory cells causes impaired glutamate release in the DLS.

To assess whether conditional RIM1 KO altered evoked neurotransmission, we measured EPSCs in DLS MSNs in response to electrical stimulation at the callosal-DLS border (Fig. 4A). Stimulation across a range of intensities revealed a significant reduction in evoked EPSC amplitude in $Emx1::Cre;RIM1^{fl/fl}$ mice relative to $RIM1^{fl/fl}$ littermates (Fig. 4B; $n = 9$, $n = 11$; two-way ANOVA: current \times genotype interaction: $F_{(10,180)} = 2.557$, $p < 0.01$), indicative of an impairment in evoked excitatory transmission.

To test whether the changes in corticostriatal neurotransmission following RIM1 KO could be attributed to changes in presynaptic release probability, we assessed the ratio of excitatory synaptic responses to pairs of closely timed electrical pulses (paired pulse ratio) in DLS MSNs of $Emx1::Cre;RIM1^{fl/fl}$ and $RIM1^{fl/fl}$ mice. Paired pulse facilitation was enhanced in $Emx1::Cre;RIM1^{fl/fl}$ mice relative to $RIM1^{fl/fl}$ littermates (Fig. 4C; $n = 15$, $n = 11$; genotype: $F_{(1,24)} = 7.825$, $p < 0.05$; IPI \times genotype interaction: $F_{(6,144)} = 2.997$, $p < 0.01$), particularly at short in-

terpulses intervals (20 ms, $p < 0.001$; 40 ms, $p < 0.05$). Because paired pulse facilitation is normally inversely correlated with neurotransmitter release probability (Thomson, 2000), this finding suggests that transmitter release probability is lower at corticostriatal synapses lacking RIM1.

We also measured the adaptation of synaptic responses during short trains of moderate frequency stimulation (5–10 Hz) to further assess how transmission and use-dependent short-term plasticity are impaired following conditional deletion of RIM1. $RIM1^{fl/fl}$ and $Emx1::Cre;RIM1^{-/-}$ mice showed no difference in the depression of EPSC amplitude observed across a 2 s, 5 Hz train (data not shown); however, relative to $RIM1^{fl/fl}$ mice, $Emx1::Cre;RIM1^{-/-}$ mice showed a resistance to the depression observed across a 2 s, 10 Hz train (Fig. 4D; $n = 13$, $n = 12$; main effect of stimulus: $F_{(19,437)} = 34.50$, $p < 0.001$; main effect of genotype: $F_{(1,23)} = 7.143$, $p < 0.05$; stimulus \times genotype interaction: $F_{(19,437)} = 1.832$, $p < 0.05$). These findings are further consistent with a use-dependent impairment in synaptic transmission at corticostriatal synapses.

Spared forms of short- and long-term plasticity at corticostriatal synapses in conditional RIM1 KO mice

To assess whether corticostriatal RIM1 was necessary for presynaptic GPCR-mediated forms plasticity in the DLS (Lovinger, 2010), we first tested $RIM1^{fl/fl}$ and $Emx1::Cre;RIM1^{-/-}$ mice for DSE, an effect mediated by short-term endocannabinoid signaling at CB1Rs on striatal glutamatergic terminals (Shonesy et al., 2013). DSE was intact and of similar magnitude and duration in slices from conditional RIM1 KO and control mice (Fig. 5A; $n = 10$, $n = 10$; unpaired t test [on amplitude of first EPSC following depolarization]; $t_{(18)} = 0.154$, $p = 0.880$).

We then assessed whether endocannabinoid/CB1R-mediated LTD of excitatory transmission in the DLS, induced by treatment with DHPG (Kreitzer and Malenka, 2005), was intact in conditional RIM1 KO mice. $RIM1^{fl/fl}$ and $Emx1::Cre;RIM1^{-/-}$ mice showed comparable DHPG-induced LTD (Fig. 5B; $n = 7$, $n = 8$; unpaired t test [on average EPSC amplitude during final 10 min]; $t_{(13)} = 1.212$, $p = 0.247$). Pretreatment with the CB1R antagonist, AM251, confirmed that DHPG-induced LTD in both groups of mice required activation of this presynaptic receptor (Fig. 5C; DHPG vs AM251+DHPG in $Emx1::Cre;RIM1^{-/-}$ mice; $n = 6$, $n = 8$; unpaired t test [on average EPSC amplitude during final 10 min]; $t_{(12)} = 2.445$, $p < 0.05$; DHPG vs AM251+DHPG in $RIM1^{fl/fl}$ mice; $n = 7$, $n = 7$; unpaired t test; $t_{(12)} = 1.278$, $p = 0.128$; DHPG alone in $RIM1^{fl/fl}$ mice; $n = 7$; one-sample t test, against baseline of 100; $t_{(6)} = 4.148$, $p < 0.001$; AM251+DHPG

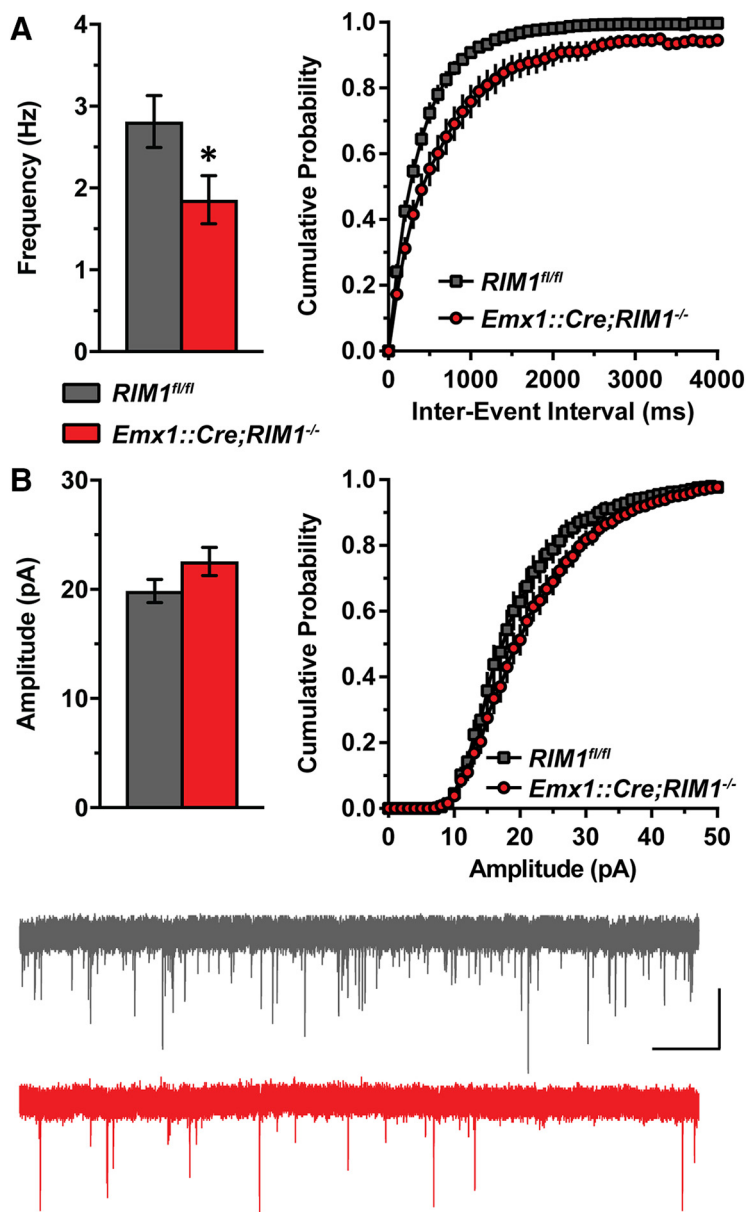


Figure 3. Impaired spontaneous excitatory synaptic transmission in DLS of conditional RIM1 KO mice. **A**, Average and cumulative probability plots of frequency and interevent interval of sEPSCs in DLS of $RIM1^{fl/fl}$ and $Emx1::Cre;RIM1^{-/-}$ mice. **B**, Average and cumulative probability plots of amplitude of sEPSCs in DLS of $RIM1^{fl/fl}$ and $Emx1::Cre;RIM1^{-/-}$ mice. * $p < 0.05$, different from $RIM1^{fl/fl}$ group. Calibration: 2 s, 20 pA.

in $RIM1^{fl/fl}$ mice; $n = 7$; one-sample t test; $t_{(6)} = 1.217$, $p = 0.269$). Demonstrating that the lack of effect of conditional RIM1 deletion on long-term forms of plasticity extended beyond LTD mediated through CB1Rs, we found that LTD induced by the mGlu_{2/3} receptor agonist LY379268 was indistinguishable in $RIM1^{fl/fl}$ and $Emx1::Cre;RIM1^{-/-}$ mice (Fig. 5D; $n = 4$, $n = 7$; unpaired t test [on average EPSC amplitude during final 10 min]; $t_{(9)} = 1.181$, $p = 0.268$). Together, these findings indicate that RIM1 within cortical inputs to the DLS is necessary for normal corticostriatal transmission, but not for several forms of short- and long-term presynaptic plasticity.

Transiently enhanced homecage locomotion in conditional RIM1 KO mice

Given this synaptic phenotype in a brain region critical for action learning and control, we next evaluated conditional RIM1 KO

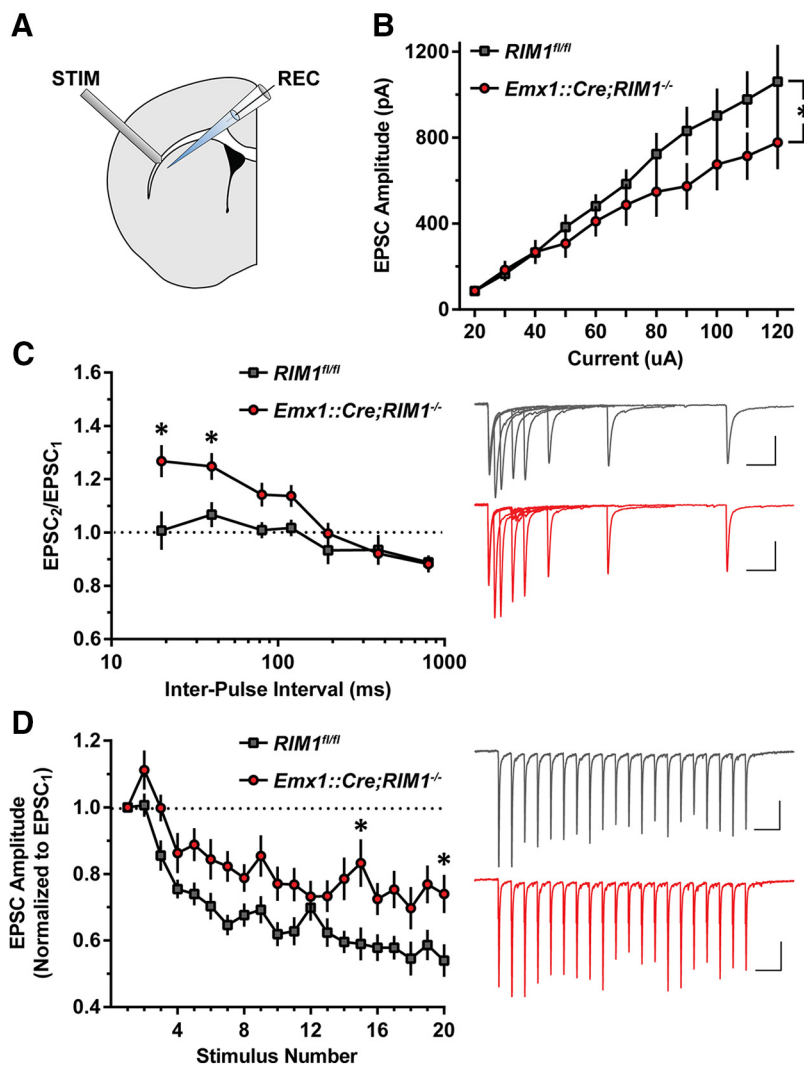


Figure 4. Impaired evoked excitatory synaptic transmission in DLS of conditional RIM1 KO mice. **A**, Schematic diagram of stimulating and recording electrode placement in DLS. **B**, Input–output curves of electrically evoked excitatory currents in DLS of *RIM1^{fl/fl}* and *Emx1::Cre;RIM1^{-/-}* mice. **C**, Paired pulse ratios of electrically evoked excitatory transmission in DLS of *RIM1^{fl/fl}* and *Emx1::Cre;RIM1^{-/-}* mice. **D**, Activity-dependent depression during 10 Hz train of electrical stimulation at border of DLS in *RIM1^{fl/fl}* and *Emx1::Cre;RIM1^{-/-}* mice. * $p < 0.05$, different from *RIM1^{fl/fl}* group. Calibration: **C**, 100 ms, 100 pA; **D**, 200 ms, 100 pA.

mice for associated behavioral deficits. *RIM1^{fl/fl}* and *Emx1::Cre;RIM1^{-/-}* mice were first assessed for differences in basal locomotion in their homecages for 24 h/d for 3 d. Mice were placed into a homecage with fresh bedding 1 h into the dark period. *Emx1::Cre;RIM1^{-/-}* mice showed enhanced locomotion during the first dark period relative to their *RIM1^{fl/fl}* littermates, but this diminished to control levels by the first light period (Fig. 6A–C; $n = 8$, $n = 13$; hierarchical linear mixed model; main effect of day: $F_{(2,95)} = 29.153$, $p < 0.001$; main effect of genotype: $F_{(1,19)} = 1.302$, $p = 0.268$; light \times day interaction: $F_{(3,95)} = 105.721$, $p < 0.0001$; day \times genotype interaction: $F_{(2,95)} = 1.306$, $p = 0.276$; light \times day \times genotype interaction: $F_{(3,95)} = 3.701$, $p = 0.014$; day 1, dark, *RIM1^{fl/fl}* vs *Emx1::Cre;RIM1^{-/-}*, $p < 0.01$).

Novelty-induced hyperactivity in conditional RIM1 KO mice

To further characterize this hyperactivity phenotype, *Emx1::Cre;RIM1^{-/-}* and *RIM1^{fl/fl}* mice were tested for locomotion during the light period in a novel cage for 2 h/d for 6 d. One cohort of mice had their testing cages replaced with a clean cage daily, and

a different cohort had their cages left unchanged for the 6 d period. *Emx1::Cre;RIM1^{-/-}* mice whose cages were changed daily showed enhanced locomotion on day 1 that gradually converged with levels seen in *RIM1^{fl/fl}* littermate controls by day 4 (Fig. 6D,E; $n = 11$, $n = 12$; two-way ANOVA; main effect of genotype: $F_{(1,21)} = 6.976$, $p < 0.05$; day \times genotype interaction: $F_{(5,105)} = 8.130$, $p < 0.001$; *RIM1^{fl/fl}* vs *Emx1::Cre;RIM1^{-/-}*, day 1: $p < 0.001$; day 2: $p < 0.05$; day 3: $p < 0.05$). Importantly, these locomotor effects were not driven by Cre expression alone because *Emx1::Cre* mice showed normal locomotion in a novel cage (Fig. 6F; $n = 9$, $n = 9$; two-way ANOVA; main effect of genotype: $F_{(1,16)} = 0.011$, $p = 0.919$). *Emx1::Cre;RIM1^{-/-}* mice whose cages were left unchanged showed initially enhanced locomotion that reduced to control levels by day 2 (Fig. 6G,H; $n = 10$, $n = 11$; two-way ANOVA; main effect of genotype: $F_{(1,19)} = 0.863$, $p = 0.365$; day \times genotype interaction: $F_{(5,95)} = 9.086$, $p < 0.001$; *RIM1^{fl/fl}* vs *Emx1::Cre;RIM1^{-/-}*, day 1: $p < 0.05$). Together, these findings suggest that *Emx1::Cre;RIM1^{-/-}* mice show novelty-induced hyperactivity.

To assess sex differences in this hyperactivity, we combined data collected on locomotor test day 1 from both experimental cohorts (those whose cages were subsequently changed or unchanged). Male and female *Emx1::Cre;RIM1^{-/-}* mice showed comparable novelty-induced hyperactivity relative to their *RIM1^{fl/fl}* littermates (males, $n = 11$, $n = 10$; females, $n = 10$, $n = 13$; two-way ANOVA; main effect of sex: $F_{(1,40)} = 1.21$, $p = 0.278$; main effect of genotype: $F_{(1,40)} = 20.57$, $p < 0.0001$; sex \times genotype interaction: $F_{(1,40)} = 2.841$, $p = 0.10$). The

novelty-induced hyperactivity seen here parallels that seen in global *RIM1 α* KO mice (Blundell et al., 2010) and mice with conditional RIM1 KO driven by the kainate receptor subunit 1 promoter (Haws et al., 2012). Notably, *Emx1::Cre;RIM1^{-/-}* mice did not recapitulate every phenotype seen in global *RIM1 α* KO mice, including impairments in prepulse inhibition (Fig. 6I; $n = 10$, $n = 10$; two-way ANOVA; main effect of genotype: $F_{(1,18)} = 0.079$, $p = 0.781$) (Blundell et al., 2010).

Impaired motor skill learning in conditional RIM1 KO mice

In a further phenotypic departure from global *RIM1 α* mice (Powell et al., 2004), *Emx1::Cre;RIM1^{-/-}* mice showed impaired performance on the accelerating rotarod relative to their *RIM1^{fl/fl}* littermates (Fig. 7; $n = 16$, $n = 15$; hierarchical linear mixed model; main effect of day: $F_{(3,319)} = 39.759$, $p < 0.0001$; main effect of genotype: $F_{(1,29)} = 4.411$, $p < 0.05$; trial \times day interaction, $F_{(8,319)} = 12.067$, $p < 0.0001$). Male and female *Emx1::Cre;RIM1^{-/-}* mice showed comparable deficits in overall rotarod performance relative to their *RIM1^{fl/fl}* littermates (males, $n = 10$,

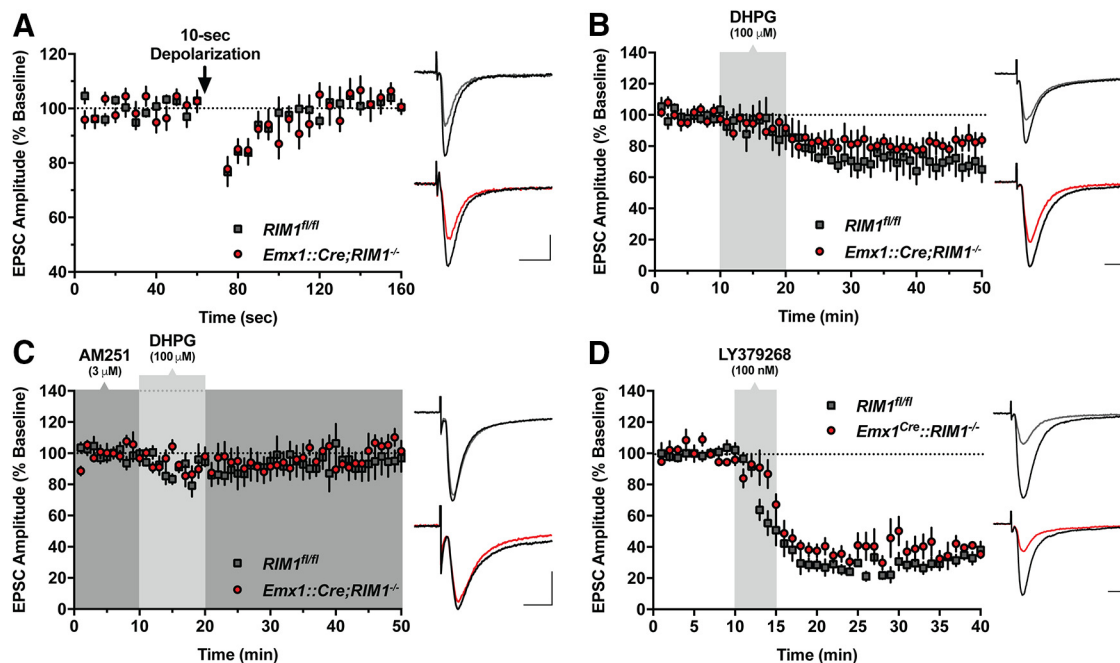


Figure 5. Intact short- and long-term depression of excitatory synaptic transmission in conditional RIM1 KO mice. **A**, DSE in DLS of *RIM1^{fl/fl}* and *Emx1::Cre;RIM1^{-/-}* mice. Arrow indicates 10 s period of postsynaptic depolarization to 0 mV. **B**, DHPG-induced LTD of EPSCs in DLS of *RIM1^{fl/fl}* and *Emx1::Cre;RIM1^{-/-}* mice. **C**, Effects of CB1R antagonist AM251 preincubation on DHPG-mediated LTD of EPSCs in DLS of *RIM1^{fl/fl}* and *Emx1::Cre;RIM1^{-/-}* mice. **D**, LTD of EPSCs in DLS of *RIM1^{fl/fl}* and *Emx1::Cre;RIM1^{-/-}* mice induced by bath application of mGlu_{2/3} receptor agonist, LY379268. Calibration: 10 ms, 100 pA.

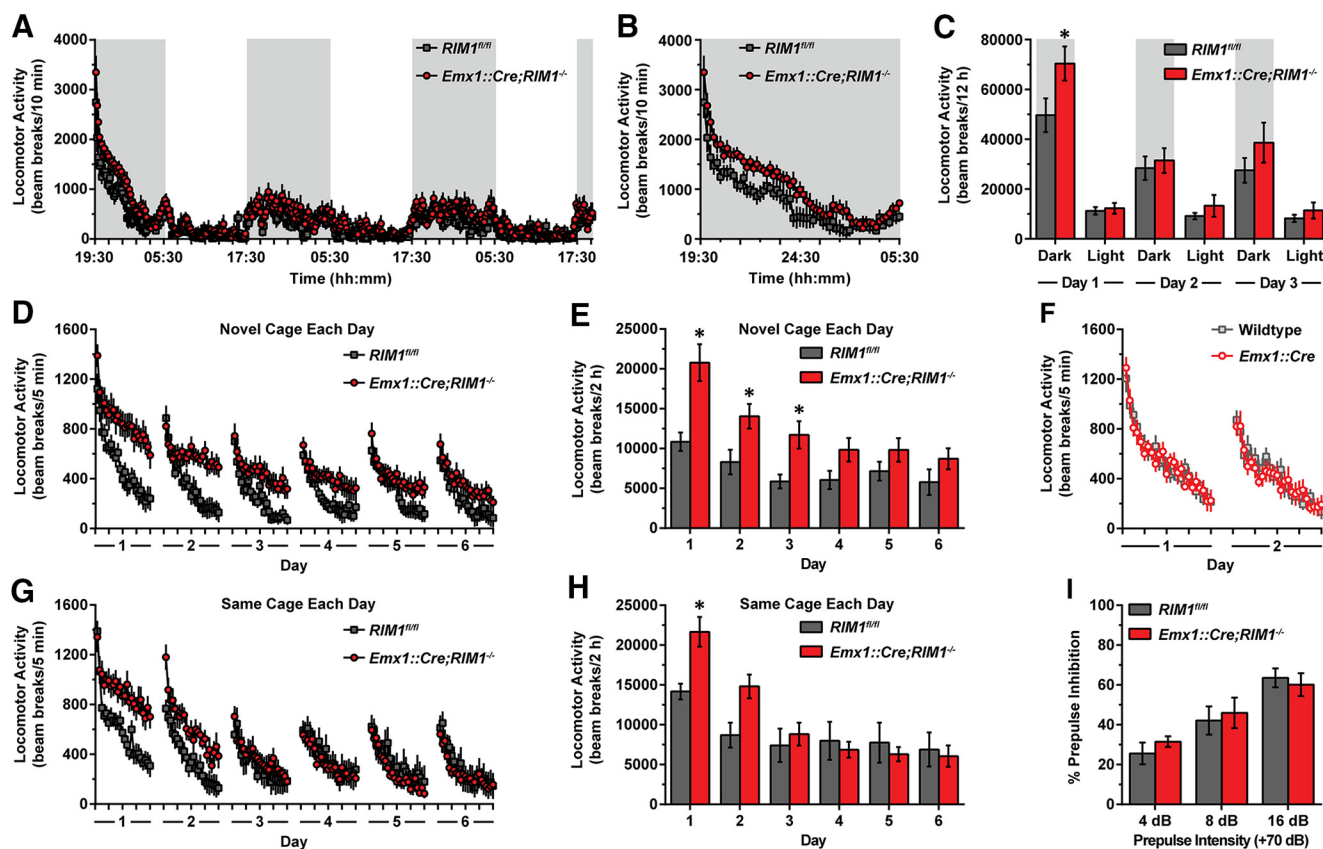


Figure 6. Enhanced novelty-induced locomotion in conditional RIM1 KO mice. **A–C**, Homecage locomotion in *RIM1^{fl/fl}* and *Emx1::Cre;RIM1^{-/-}* across 3 d. Novelty-induced locomotion was observed in the first 10 h following exposure to the novel homecage (**B**). **D, E**, Novelty-induced locomotion in *RIM1^{fl/fl}* and *Emx1::Cre;RIM1^{-/-}* mice in 10 min (**D**) or 120 min bins (**E**) when fresh bedding and a new locomotor chamber were introduced daily. **F**, No novelty-induced hyperactivity was observed in *Emx1::Cre* mice. **G, H**, Novelty-induced locomotion in *RIM1^{fl/fl}* and *Emx1::Cre;RIM1^{-/-}* mice in 10 min (**G**) or 120 min bins (**H**) when cages were unchanged across 6 d of locomotor testing. **p* < 0.05, different from *RIM1^{fl/fl}* group. **I**, Prepulse inhibition in *RIM1^{fl/fl}* and *Emx1::Cre;RIM1^{-/-}* mice.

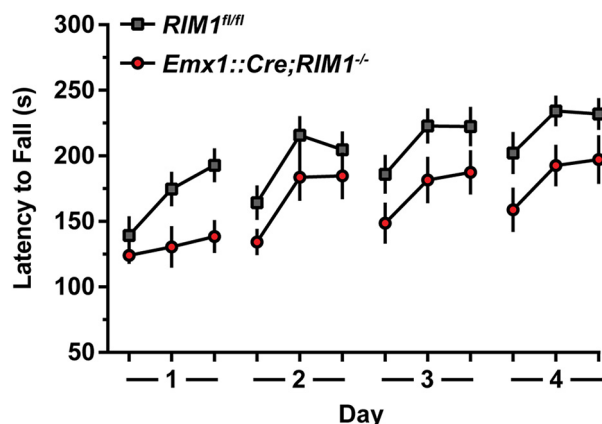


Figure 7. Impaired motor learning in conditional RIM1 KO mice. Latency to fall from the accelerating rotarod in *RIM1^{fl/fl}* and *Emx1::Cre;RIM1^{-/-}* mice. * $p < 0.05$, different from *RIM1^{fl/fl}* group.

$n = 10$; females, $n = 6$, $n = 5$; two-way ANOVA; main effect of sex: $F_{(1,27)} = 2.616$, $p = 0.117$; main effect of genotype: $F_{(1,27)} = 4.617$, $p < 0.05$; sex \times genotype interaction: $F_{(1,27)} = 0.3521$, $p = 0.558$). These findings suggest that cortical RIM1 may be particularly important for aspects of action learning, including the refinement of actions into motor skills.

Heightened responding on FR and PR schedules in conditional RIM1 KO mice

We next assessed whether RIM1-dependent processes in forebrain excitatory neurons were required for normal instrumental learning. *RIM1^{fl/fl}* and *Emx1::Cre;RIM1^{-/-}* mice were food restricted and trained to lever press for food pellets on escalating FR schedules of reinforcement. Both groups pressed the “active” lever sufficient numbers of times to receive all allotted food pellets each day (Fig. 8A). However, *Emx1::Cre;RIM1^{-/-}* mice showed heightened rates of responding for food during the higher FR sessions (Fig. 8B; $n = 14$, $n = 12$; two-way ANOVA; main effect of genotype: $F_{(1,24)} = 6.063$, $p < 0.05$; day \times genotype interaction: $F_{(8,192)} = 4.519$, $p < 0.001$; *RIM1^{fl/fl}* vs *Emx1::Cre;RIM1^{-/-}*, day 8 and 9: $p < 0.05$). *Emx1::Cre;RIM1^{-/-}* mice also showed temporarily heightened numbers of head entries into the food dispenser early in instrumental training (Fig. 8C; $n = 11$, $n = 11$; two-way ANOVA; day \times genotype interaction: $F_{(8,160)} = 2.076$, $p < 0.05$; *RIM1^{fl/fl}* vs *Emx1::Cre;RIM1^{-/-}*, day 2: $p < 0.05$). These behavioral differences were not attributable to differences in body weight responses to food restriction (Fig. 8D) or to general differences in propensity for consumption, as *RIM1^{fl/fl}* and *Emx1::Cre;RIM1^{-/-}* mice ate comparable amounts of food during subsequent post testing *ad libitum* access to food pellets in their homecages (*RIM1^{fl/fl}*, 6.27 ± 0.34 g vs *Emx1::Cre;RIM1^{-/-}*, 6.66 ± 0.23 g). Heightened responding also did not simply reflect general hyperactivity as average daily inactive lever pressing rates were statistically indistinguishable across groups (two-way ANOVA; main effect of genotype: $F_{(1,24)} = 0.882$, $p = 0.357$) and press counts were consistently low across all training sessions (*RIM1^{fl/fl}*, 5.18 ± 1.50 presses vs *Emx1::Cre;RIM1^{-/-}*, 7.31 ± 1.83 presses).

Mice subsequently underwent a PR test in which they were required to press the active lever a progressively increasing number of times to receive a food pellet. Relative to littermate *RIM1^{fl/fl}* controls, *Emx1::Cre;RIM1^{-/-}* mice showed heightened active lever pressing for food during this test (Fig. 8E; unpaired t test;

$t_{(24)} = 3.295$, $p < 0.005$), and obtained higher breakpoints in their responding (Fig. 8F; Mann–Whitney test; $U = 26$, $p < 0.005$). Male and female *Emx1::Cre;RIM1^{-/-}* mice showed comparably enhanced active lever pressing during the PR test relative to their *RIM1^{fl/fl}* littermates (males, $n = 7$, $n = 8$; females, $n = 5$, $n = 6$; two-way ANOVA; main effect of sex: $F_{(1,22)} = 1.13$, $p = 0.299$; main effect of genotype: $F_{(1,22)} = 6.505$, $p < 0.05$; sex \times genotype interaction: $F_{(1,22)} = 0.020$, $p = 0.888$). Responding on the inactive lever during the PR test was also elevated in *Emx1::Cre;RIM1^{-/-}* relative to *RIM1^{fl/fl}* mice ($t_{(24)} = 2.703$, $p < 0.05$), but inactive lever responding was consistently low relative to active lever responding in both groups ($8.06 \pm 3.53\%$ and $8.67 \pm 1.38\%$ in *RIM1^{fl/fl}* and *Emx1::Cre;RIM1^{-/-}* mice, respectively). These results indicate that conditional RIM1 KO mice show heightened instrumental responding for food, most prominently under higher-effort conditions.

Enhanced responding on RI schedules and resistance to developing habitual actions in conditional RIM1 KO mice

Action strategies used during instrumental learning and responding have been shown to exist on a gradient between outcome-dependent/goal-directed and outcome-independent/habitual. To delineate the action strategy used by *Emx1::Cre;RIM1^{-/-}* mice during food responding, we trained a cohort of *Emx1::Cre;RIM1^{-/-}* and *RIM1^{fl/fl}* mice on escalating RI schedules of reinforcement known to bias learning toward the use of habitual response strategies (Dickinson, 1985; Gremel and Costa, 2013). RI schedules promote habitual responding by weakening the contingency and contiguity between the action (lever press) and outcome (food pellet) (Dickinson, 1985; Derusso et al., 2010). To assess their propensity to use a goal-directed or habitual action strategy, mice underwent sensory-specific satiety outcome devaluation testing over two consecutive days, termed valued and devalued days. Mice were permitted 1 h *ad libitum* consumption of either a familiar sucrose solution on the “valued” day, and food pellets previously earned by lever pressing on the “devalued” day, each followed by a 5 min period of nonrewarded lever pressing. A larger reduction in lever pressing in the devalued versus the valued state is indicative of greater goal-directed action control; indistinguishable lever pressing in the devalued and valued states is indicative of habitual control (Dickinson, 1985; Gremel et al., 2016).

Relative to *RIM1^{fl/fl}* mice, *Emx1::Cre;RIM1^{-/-}* mice showed heightened levels of responding (Fig. 9A; $n = 16$, $n = 14$; two-way ANOVA; day \times genotype interaction: $F_{(9,252)} = 2.726$, $p < 0.005$; *RIM1^{fl/fl}* vs *Emx1::Cre;RIM1^{-/-}*, day 9 and 10, $p < 0.05$) and rates of responding for food during high RI training (Fig. 9B; day \times genotype interaction: $F_{(9,252)} = 2.787$, $p < 0.005$; *RIM1^{fl/fl}* vs *Emx1::Cre;RIM1^{-/-}*, day 10, $p < 0.05$). As seen in the cohort of mice trained on escalating FR schedules, *Emx1::Cre;RIM1^{-/-}* mice showed transiently elevated numbers of head entries early in instrumental training (Fig. 9C; $n = 15$, $n = 10$; two-way ANOVA; day \times genotype interaction: $F_{(9,207)} = 2.016$, $p < 0.05$; *RIM1^{fl/fl}* vs *Emx1::Cre;RIM1^{-/-}*, day 1: $p < 0.05$). Again, this heightened responding was not attributable to genotype differences in body weight responses to food restriction (data not shown).

Devaluation testing revealed that *RIM1^{fl/fl}* mice responded comparably on the valued and devalued days (Fig. 9D; two-way ANOVA; valuation \times genotype interaction: $F_{(1,28)} = 5.862$, $p < 0.05$; valued vs devalued, *RIM1^{fl/fl}*: $p = 0.428$), consistent with the expected use of a habitual action strategy following RI schedule training. In contrast, *Emx1::Cre;RIM1^{-/-}* mice showed reduced lever pressing on the devalued day relative to the valued day (Fig.

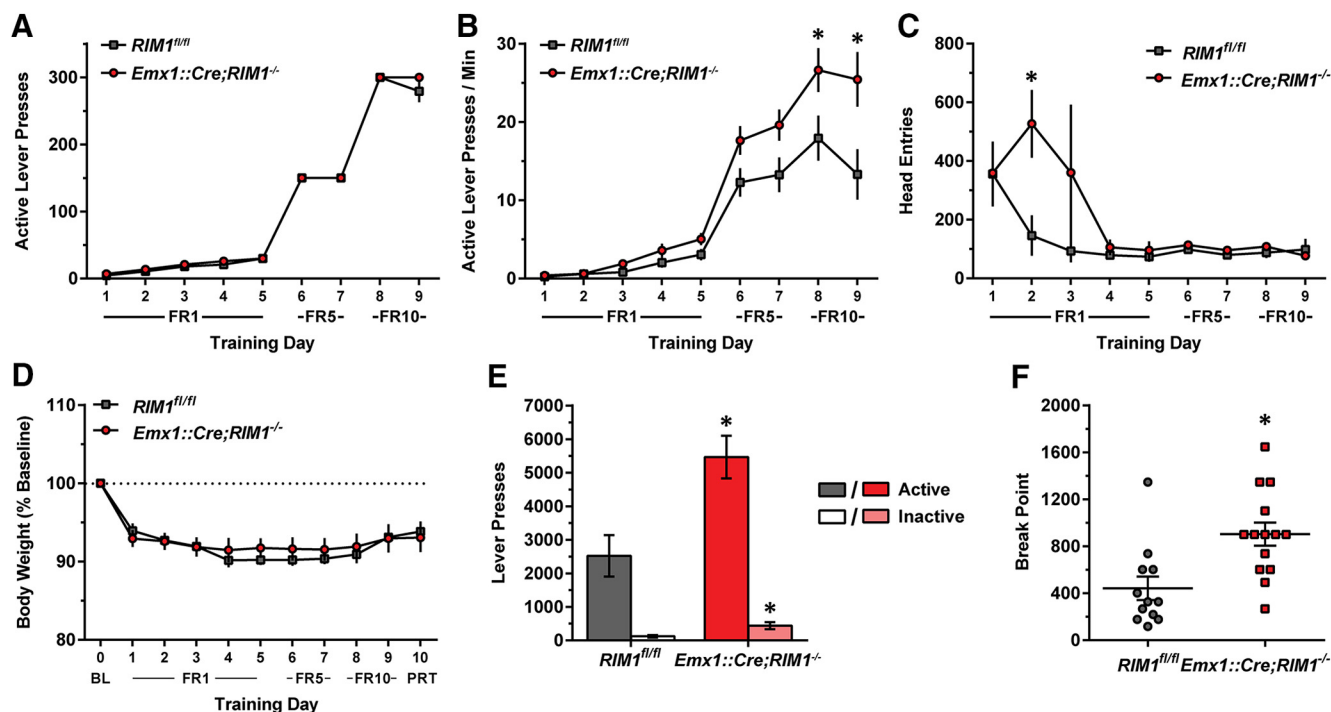


Figure 8. Enhanced instrumental responding for food in conditional RIM1 KO mice. **A, B**, Active lever presses (**A**), active lever presses/min (**B**), and head entries into the food receptacle (**C**) during FR schedule training in *RIM1^{fl/fl}* and *Emx1::Cre;RIM1^{-/-}* mice. **D**, Body weight response to food restriction across training. **E, F**, Active and inactive lever presses (**E**) and breakpoints achieved (**F**) during PR testing in *RIM1^{fl/fl}* and *Emx1::Cre;RIM1^{-/-}* mice. * $p < 0.05$, different from *RIM1^{fl/fl}* group.

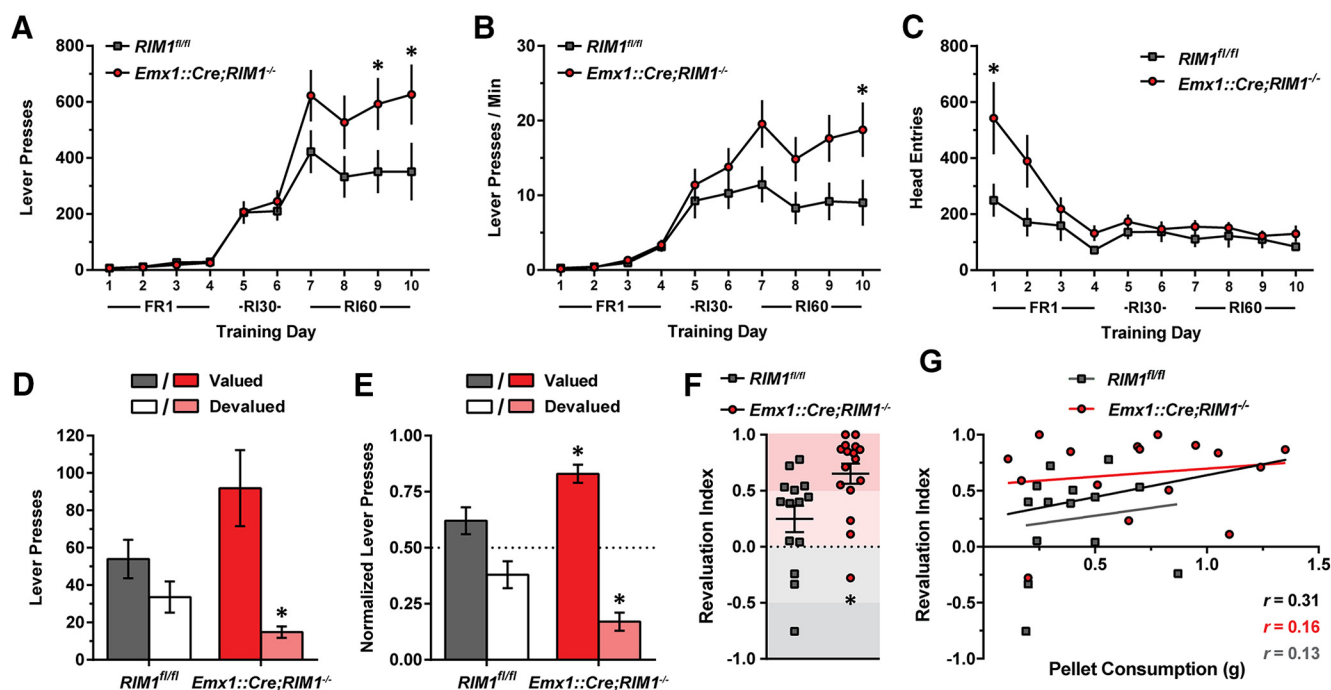


Figure 9. Impaired habitual responding for food in conditional RIM1 KO mice. **A, B**, Lever presses (**A**), lever presses/min (**B**), and head entries into the food receptacle (**C**) during FR and RI schedule training in *RIM1^{fl/fl}* and *Emx1::Cre;RIM1^{-/-}* mice. **D**, Lever presses during valuation testing in *RIM1^{fl/fl}* and *Emx1::Cre;RIM1^{-/-}* mice. * $p < 0.05$, different from valued condition. **E**, Normalized lever presses during valuation testing in *RIM1^{fl/fl}* and *Emx1::Cre;RIM1^{-/-}* mice. * $p < 0.05$, different from 0.50. **F**, Revaluation index in response to valuation testing in *RIM1^{fl/fl}* and *Emx1::Cre;RIM1^{-/-}* mice. * $p < 0.05$, different from *RIM1^{fl/fl}* group. **G**, Correlation between pellet consumption during *ad libitum* feeding and revaluation index in *RIM1^{fl/fl}* mice (gray line), *Emx1::Cre;RIM1^{-/-}* mice (red line), and both combined (black line). All correlations were nonsignificant.

9D; ANOVA [as above]; valued vs devalued, *Emx1::Cre;RIM1^{-/-}*; $p < 0.05$). Analysis of normalized lever pressing during valued and devalued conditions revealed that *Emx1::Cre;RIM1^{-/-}*, but not *RIM1^{fl/fl}*, mice were significantly sensitive to

devaluation (Fig. 9E; one-sample t test, against “no devaluation” point of 0.5; *Emx1::Cre;RIM1^{-/-}*; $t_{(15)} = 7.293$, $p < 0.0001$; *RIM1^{fl/fl}*; $t_{(13)} = 2.119$, $p = 0.054$). Notably, devaluation in *RIM1^{fl/fl}* mice narrowly avoided significance, indicative of mod-

est expression of a habitual action strategy in these mice. Significant sensitivity to devaluation was seen in male and female *Emx1::Cre;RIM1^{-/-}* mice (males, $n = 7$: $t_{(6)} = 7.901$, $p < 0.0005$; females, $n = 9$: $t_{(8)} = 4.136$, $p < 0.005$), but not male and female *RIM1^{fl/fl}* mice (males, $n = 6$: $t_{(5)} = 2.175$, $p = 0.082$; females, $n = 8$: $t_{(7)} = 1.077$, $p = 0.317$). Furthermore, using a “reevaluation index” ($[\text{Valued} - \text{Devalued Lever Presses}]/\text{Total Lever Presses}$) as a measure of goal-directedness (Gremel and Costa, 2013; Gremel et al., 2016), we found that *Emx1::Cre;RIM1^{-/-}* mice showed greater goal-directedness than their *RIM1^{fl/fl}* littermates (Fig. 9F; $t_{(28)} = 2.774$, $p < 0.01$). Notably, despite consuming comparable amounts of sucrose as *RIM1^{fl/fl}* mice during the 1 h *ad libitum* feeding session preceding valuation testing (0.92 ± 0.16 vs 0.79 ± 0.13 g, $t_{(28)} = 0.612$, $p = 0.546$), *Emx1::Cre;RIM1^{-/-}* mice consumed more food pellets than *RIM1^{fl/fl}* mice during the corresponding prefeeding session (0.69 ± 0.10 vs 0.40 ± 0.06 g, $t_{(28)} = 2.459$, $p = 0.020$). However, no correlation was observed between pellet consumption and reevaluation index in either group of mice (Fig. 9G), suggesting that variation in pellet consumption did not meaningfully impact devaluation of responding for pellets. Together, these data indicate that RIM1-dependent processes in cortical excitatory neurons may help to constrain goal-directed action and contribute to the learning and/or use of habits.

Discussion

Here we combine genetic, electrophysiological, and behavioral approaches to assess presynaptic processes within corticostriatal projections that subserve normal action learning and control. We show that conditional deletion of RIM1 presynaptic scaffold proteins from corticostriatal projection neurons (and other forebrain excitatory neurons) impairs excitatory transmission in the DLS but spares many forms of presynaptic GPCR-mediated short- and long-term striatal plasticity. Conditional RIM1 KO mice show elevated locomotor responses to novelty and impaired motor learning on the accelerating rotarod. They further show abnormally robust goal-directed responding for food. These findings implicate RIM1-dependent processes in corticostriatal transmission and in the learning and control of motivated behavior.

The selective effect of RIM1 deletion on corticostriatal transmission (not CB1R- or mGlu_{2/3} receptor-mediated plasticity), although unexpected, is consistent with selective roles for RIM1-dependent processes in transmission or plasticity at other central synapses (Castillo et al., 2002; Schoch et al., 2002; Lonart et al., 2003; Abrahamsson et al., 2017). Global deletion of RIM1 α has been shown to attenuate DHPG-induced LTD of excitatory transmission in the nucleus accumbens (Grueter et al., 2010); however, unlike in the present study, the terminal population driving the effect of this single isoform deletion is unclear. Furthermore, plasticity mechanisms are well documented to be differentiable in dorsal and ventral striatum subregions (Lovinger, 2010; Russo et al., 2010). Although it is possible that the lack of effect of RIM1 deletion on GPCR-mediated forms of plasticity resulted from recruitment of DLS inputs derived from populations of non-*Emx1::Cre* (and therefore RIM1-expressing) neurons, we believe this interpretation to be unlikely. First, Cre expression in *Emx1::Cre* mice drives recombination in the vast majority (~88%) of cortical pyramidal neurons (Gorski et al., 2002). Indeed, we observed robust Cre-mediated knockdown of RIM1 mRNA in M1 and M2 motor cortices that densely innervate the DLS (Fig. 1A). Second, the other principle source of excitatory inputs to the DLS is the thalamus (Hunnicutt et al.,

2014, 2016), but the synaptic properties (e.g., paired pulse ratios) of the mixed striatal inputs stimulated in the present study more closely mimicked those of cortical rather than thalamic origin (Ding et al., 2008). Moreover, thalamostriatal inputs exhibit minimal CB1R expression and CB1R-mediated forms of plasticity (Wu et al., 2015; for mGlu₂ receptor-mediated thalamostriatal plasticity, see Johnson et al., 2017). Therefore, effects of RIM1 deletion on presynaptic GPCR-mediated forms of corticostriatal plasticity are unlikely to be blunted by recruitment of RIM1-expressing DLS inputs.

Conditional RIM1 deletion from cortical pyramidal neurons favored, and intensified, the use of goal-directed action strategies during instrumental responding for food. These findings, in conjunction with the observed impairment in excitatory transmission in the DLS, support the view that the normal learning and use of habitual action strategies depend on DLS engagement (Yin et al., 2004; Dias-Ferreira et al., 2009; Thorn et al., 2010; Smith and Graybiel, 2013). In this way, weakened excitatory drive of the DLS may bias animals toward the adoption of goal-directed strategies that are more reliant on dorsomedial striatum-based circuitry (Yin et al., 2005b; Gremel and Costa, 2013; Hart et al., 2018). Of course, in the present study, RIM1 was deleted from widespread cortical structures, including from associative and limbic cortical regions that innervate the dorsomedial striatum and ventral striatum (McGeorge and Faull, 1989; Hintiryan et al., 2016). Deletion-induced impairments in excitatory transmission may also occur in these and other regions and contribute to the array of behavioral phenotypes observed in these animals. It remains notable, however, that widespread cortical RIM1 deletion led to a net bias toward goal-directed actions. Future work mapping the synaptic phenotypes seen across striatal subregions following cortical RIM1 deletion would help to explain this net bias.

A major impetus for targeting electrophysiology recordings to the DLS was to explore the relationship between prominent forms of DLS presynaptic plasticity and action control. Indeed, prior work has proposed that CB1R-mediated LTD in the DLS plays an important role in habit expression because the two phenomena are impaired following the development of tolerance to a CB1R agonist (Δ^9 -THC) and are rescued upon restoration of endocannabinoid signaling in the DLS (Nazzaro et al., 2012). The sparing of CB1R-mediated LTD in the DLS following RIM1 deletion did not permit direct testing of this hypothesis. However, it is probable that impairment of synaptic mechanisms other than LTD can interfere with habit learning even when LTD is normal. Indeed, multiple mechanisms are likely to contribute to over-reliance or under-reliance on DLS-based circuits that can promote or impair habit learning and use (Corbit et al., 2014; Barker et al., 2015; Gremel et al., 2016; O'Hare et al., 2017). Variation in CB1R-mediated plasticity in the DLS is only one such mechanism.

Motor skill learning was also found to be impaired following cortex-wide conditional RIM1 deletion. Global RIM1 α KO mice showed no such impairment across a single-day rotarod training paradigm (Powell et al., 2004), but distinct methodologies (e.g., single isoform deletion, developmental compensation, extent of training, etc.) may account for these distinct behavioral phenotypes. Our evidence of impaired motor learning, paired with a deficit in DLS excitatory transmission, supports the view that like habitual responding the learning of stereotyped motor actions depends on DLS engagement (Miyachi et al., 2002; Floyer-Lea and Matthews, 2005; Yin et al., 2009). Indeed, recent work from our group showed that sensorimotor cortical inputs to DLS are robustly engaged from the outset of action learning, and incre-

mentally disengage as actions become refined and stereotyped (Kupferschmidt et al., 2017). Findings from our group further show that conditional deletion of CB1R from cortical pyramidal neurons (in *Emx1::Cre;CB1R^{-/-}* mice) has no effect on rotarod learning (D.A.K. and D.M.L., unpublished observations). Together, these findings suggest that basal glutamate release at corticostriatal synapses (and associated postsynaptic plasticity), and not presynaptic GPCR modulation of this release, is particularly critical for motor skill learning. As above, synaptic impairments following cortical RIM1 deletion undoubtedly extend beyond those presently observed in the DLS and may contribute to the observed motor skill learning deficit.

Last, mice with the conditional RIM1 deletion showed a pronounced enhancement of the locomotor response to a novel environment. A similar enhancement was seen in global RIM1 α mice (Powell et al., 2004; Blundell et al., 2010), suggesting that RIM1 α -dependent processes in forebrain excitatory neurons contribute to this behavioral phenotype. Haws et al. (2012) showed a modest increase in novelty-induced locomotion in mice with RIM1 conditionally deleted from nearly all hippocampal CA3 pyramidal neurons plus sparse populations in dentate gyrus, cerebellum, cortex, and thalamus. Therefore, the RIM1-lacking neurons driving the novelty response in the present experiments may be primarily localized to the hippocampus and likely differ from those driving the impaired skill learning and biased instrumental action control. Notably, however, the neural substrates underlying novelty responses and appetitive motivational processes, like those that support instrumental responding under high-effort conditions, may show greater convergence, including a shared reliance on ventral striatal brain systems (Bardo et al., 1996; Legault and Wise, 2001; Salamone et al., 2003, 2016; Lisman and Grace, 2005). Therefore, neuroadaptations in such systems may underlie the heightened novelty-induced locomotion and PR food responding seen here in conditional RIM1 KO mice.

For reasons both technical and historical, study of the neural basis of action control has focused heavily on learning-related postsynaptic adaptations in basal ganglia circuits. However, the molecular players and physiological processes at work within targeted populations of presynaptic terminals have become accessible to modern neuroscientists, and their contributions to normal and disordered action control are becoming increasingly recognized. Here we advance this effort by revealing a selective role for presynaptic RIM1 in neurotransmitter release at a key input structure of the basal ganglia and provide evidence that RIM1-dependent processes help to promote the refinement of skilled actions, constrain goal-directed behaviors, and contribute to the learning and use of habits.

References

- Abrahamsson T, Chou CY, Li SY, Mancino A, Costa RP, Brock JA, Nuro E, Buchanan KA, Elgar D, Blackman AV, Tudor-Jones A, Oyrer J, Farmer WT, Murai KK, Sjöström PJ (2017) Differential regulation of evoked and spontaneous release by presynaptic NMDA receptors. *Neuron* 96: 839–855.e5. [CrossRef Medline](#)
- Atwood BK, Kupferschmidt DA, Lovinger DM (2014) Opioids induce dissociable forms of long-term depression of excitatory inputs to the dorsal striatum. *Nat Neurosci* 17:540–548. [CrossRef Medline](#)
- Balleine BW, Delgado MR, Hikosaka O (2007) The role of the dorsal striatum in reward and decision-making. *J Neurosci* 27:8161–8165. [CrossRef Medline](#)
- Bardo MT, Donohew RL, Harrington NG (1996) Psychobiology of novelty seeking and drug seeking behavior. *Behav Brain Res* 77:23–43. [CrossRef Medline](#)
- Barker JM, Corbit LH, Robinson DL, Gremel CM, Gonzales RA, Chandler LJ (2015) Corticostriatal circuitry and habitual ethanol seeking. *Alcohol* 49:817–824. [CrossRef Medline](#)
- Barnes TD, Kubota Y, Hu D, Jin DZ, Graybiel AM (2005) Activity of striatal neurons reflects dynamic encoding and recoding of procedural memories. *Nature* 437:1158–1161. [CrossRef Medline](#)
- Blundell J, Kaeser PS, Südhof TC, Powell CM (2010) RIM1 α and interacting proteins involved in presynaptic plasticity mediate prepulse inhibition and additional behaviors linked to schizophrenia. *J Neurosci* 30: 5326–5333. [CrossRef Medline](#)
- Calabresi P, Mercuri NB, De Murtas M, Bernardi G (1990) Endogenous GABA mediates presynaptic inhibition of spontaneous and evoked excitatory synaptic potentials in the rat neostriatum. *Neurosci Lett* 118:99–102. [CrossRef Medline](#)
- Calakos N, Schoch S, Südhof TC, Malenka RC (2004) Multiple roles for the active zone protein RIM1 α in late stages of neurotransmitter release. *Neuron* 42:889–896. [CrossRef Medline](#)
- Castillo PE, Schoch S, Schmitz F, Südhof TC, Malenka RC (2002) RIM1 α is required for presynaptic long-term potentiation. *Nature* 415:327–330. [CrossRef Medline](#)
- Chevalleyre V, Heifets BD, Kaeser PS, Südhof TC, Purpura DP, Castillo PE (2007) Endocannabinoid-mediated long-term plasticity requires cAMP/PKA signaling and RIM1 α . *Neuron* 54:801–812. [CrossRef Medline](#)
- Coppola T, Magnin-Luthi S, Perret-Menoud V, Gattesco S, Schiavo G, Regazzi R (2001) Direct interaction of the Rab3 effector RIM with Ca²⁺ channels, SNAP-25, and synaptotagmin. *J Biol Chem* 276:32756–32762. [CrossRef Medline](#)
- Corbit LH, Leung BK, Balleine BW (2013) The role of the amygdala-striatal pathway in the acquisition and performance of goal-directed instrumental actions. *J Neurosci* 33:17682–17690. [CrossRef Medline](#)
- Corbit LH, Chieng BC, Balleine BW (2014) Effects of repeated cocaine exposure on habit learning and reversal by N-acetylcysteine. *Neuropsychopharmacology* 39:1893–1901. [CrossRef Medline](#)
- Costa RM, Cohen D, Nicolelis MA (2004) Differential corticostriatal plasticity during fast and slow motor skill learning in mice. *Curr Biol* 14: 1124–1134. [CrossRef Medline](#)
- Dang MT, Yokoi F, Yin HH, Lovinger DM, Wang Y, Li Y (2006) Disrupted motor learning and long-term synaptic plasticity in mice lacking NMDAR1 in the striatum. *Proc Natl Acad Sci U S A* 103:15254–15259. [CrossRef Medline](#)
- Davis MI, Crittenden JR, Feng AY, Kupferschmidt DA, Naydenov A, Stella N, Graybiel AM, Lovinger DM (2018) The cannabinoid-1 receptor is abundantly expressed in striatal striosomes and striosome-dendron bouquets of the substantia nigra. *PLoS One* 13:e0191436. [CrossRef Medline](#)
- Deng L, Kaeser PS, Xu W, Südhof TC (2011) RIM proteins activate vesicle priming by reversing autoinhibitory homodimerization of Munc13. *Neuron* 69:317–331. [CrossRef Medline](#)
- Derusso AL, Fan D, Gupta J, Shelest O, Costa RM, Yin HH (2010) Instrumental uncertainty as a determinant of behavior under interval schedules of reinforcement. *Front Integr Neurosci* 4:17. [CrossRef Medline](#)
- Dias-Ferreira E, Sousa JC, Melo I, Morgado P, Mesquita AR, Cerqueira JJ, Costa RM, Sousa N (2009) Chronic stress causes frontostriatal reorganization and affects decision-making. *Science* 325:621–625. [CrossRef Medline](#)
- Dickinson A (1985) Actions and habits: the development of behavioural autonomy. *Philos Trans R Soc Lond B Biol Sci* 308:67–78. [CrossRef](#)
- Ding J, Peterson JD, Surmeier DJ (2008) Corticostriatal and thalamostriatal synapses have distinctive properties. *J Neurosci* 28:6483–6492. [CrossRef Medline](#)
- Floyer-Lea A, Matthews PM (2005) Distinguishable brain activation networks for short- and long-term motor skill learning. *J Neurophysiol* 94: 512–518. [CrossRef Medline](#)
- Fourcaudot E, Gambino F, Humeau Y, Casassus G, Shaban H, Poulain B, Lüthi A (2008) cAMP/PKA signaling and RIM1 α mediate presynaptic LTP in the lateral amygdala. *Proc Natl Acad Sci U S A* 105:15130–15135. [CrossRef Medline](#)
- Gerdeman GL, Ronesi J, Lovinger DM (2002) Postsynaptic endocannabinoid release is critical to long-term depression in the striatum. *Nat Neurosci* 5:446–451. [CrossRef Medline](#)
- Gorski JA, Talley T, Qiu M, Puellas L, Rubenstein JL, Jones KR (2002) Cortical excitatory neurons and glia, but not GABAergic neurons, are produced in the *Emx1*-expressing lineage. *J Neurosci* 22:6309–6314. [CrossRef Medline](#)

- Graybiel AM, Grafton ST (2015) The striatum: where skills and habits meet. *Cold Spring Harb Perspect Biol* 7:a021691. [CrossRef Medline](#)
- Gremel CM, Costa RM (2013) Orbitofrontal and striatal circuits dynamically encode the shift between goal-directed and habitual actions. *Nat Commun* 4:2264. [CrossRef Medline](#)
- Gremel CM, Chancey JH, Atwood BK, Luo G, Neve R, Ramakrishnan C, Deisseroth K, Lovinger DM, Costa RM (2016) Endocannabinoid modulation of orbitostriatal circuits gates habit formation. *Neuron* 90:1312–1324. [CrossRef Medline](#)
- Grueter BA, Brasnjo G, Malenka RC (2010) Postsynaptic TRPV1 triggers cell type-specific long-term depression in the nucleus accumbens. *Nat Neurosci* 13:1519–1525. [CrossRef Medline](#)
- Han Y, Kaeser PS, Südhof TC, Schneggenburger R (2011) RIM determines Ca^{2+} channel density and vesicle docking at the presynaptic active zone. *Neuron* 69:304–316. [CrossRef Medline](#)
- Hart G, Bradfield LA, Balleine BW (2018) Prefrontal corticostriatal disconnection blocks the acquisition of goal-directed action. *J Neurosci* 38:1311–1322. [CrossRef Medline](#)
- Hawes SL, Evans RC, Unruh BA, Benkert EE, Gillani F, Dumas TC, Blackwell KT (2015) Multimodal plasticity in dorsal striatum while learning a lateralized navigation task. *J Neurosci* 35:10535–10549. [CrossRef Medline](#)
- Haws ME, Kaeser PS, Jarvis DL, Südhof TC, Powell CM (2012) Region-specific deletions of RIM1 reproduce a subset of global RIM1alpha (−/−) phenotypes. *Genes Brain Behav* 11:201–213. [CrossRef Medline](#)
- Heilbronner SR, Rodriguez-Romaguera J, Quirk GJ, Groenewegen HJ, Haber SN (2016) Circuit-based corticostriatal homologies between rat and primate. *Biol Psychiatry* 80:509–521. [CrossRef Medline](#)
- Hibino H, Pironkova R, Onwumere O, Vologodskaya M, Hudspeth AJ, Lesage F (2002) RIM binding proteins (RBPs) couple Rab3-interacting molecules (RIMs) to voltage-gated Ca^{2+} channels. *Neuron* 34:411–423. [CrossRef Medline](#)
- Hintiryan H, Foster NN, Bowman I, Bay M, Song MY, Gou L, Yamashita S, Bienkowski MS, Zingg B, Zhu M, Yang XW, Shih JC, Toga AW, Dong HW (2016) The mouse cortico-striatal projectome. *Nat Neurosci* 19:1100–1114. [CrossRef Medline](#)
- Huerta-Ocampo I, Mena-Segovia J, Bolam JP (2014) Convergence of cortical and thalamic input to direct and indirect pathway medium spiny neurons in the striatum. *Brain Struct Funct* 219:1787–1800. [CrossRef Medline](#)
- Hunnicutt BJ, Long BR, Kusefoglu D, Gertz KJ, Zhong H, Mao T (2014) A comprehensive thalamocortical projection map at the mesoscopic level. *Nat Neurosci* 17:1276–1285. [CrossRef Medline](#)
- Hunnicutt BJ, Jongbloets BC, Birdsong WT, Gertz KJ, Zhong H, Mao T (2016) A comprehensive excitatory input map of the striatum reveals novel functional organization. *Elife* 5:19103. [CrossRef Medline](#)
- Johnson KA, Mateo Y, Lovinger DM (2017) Metabotropic glutamate receptor 2 inhibits thalamically-driven glutamate and dopamine release in the dorsal striatum. *Neuropharmacology* 117:114–123. [CrossRef Medline](#)
- Kaeser PS, Kwon HB, Chiu CQ, Deng L, Castillo PE, Südhof TC (2008a) RIM1alpha and RIM1beta are synthesized from distinct promoters of the RIM1 gene to mediate differential but overlapping synaptic functions. *J Neurosci* 28:13435–13447. [CrossRef Medline](#)
- Kaeser PS, Kwon HB, Blundell J, Chevaleyre V, Morishita W, Malenka RC, Powell CM, Castillo PE, Südhof TC (2008b) RIM1alpha phosphorylation at serine-413 by protein kinase A is not required for presynaptic long-term plasticity or learning. *Proc Natl Acad Sci U S A* 105:14680–14685. [CrossRef Medline](#)
- Kaeser PS, Deng L, Wang Y, Dulubova I, Liu X, Rizo J, Südhof TC (2011) RIM proteins tether Ca^{2+} channels to presynaptic active zones via a direct PDZ-domain interaction. *Cell* 144:282–295. [CrossRef Medline](#)
- Kelley AE, Domesick VB, Nauta WJ (1982) The amygdalostriatal projection in the rat—an anatomical study by anterograde and retrograde tracing methods. *Neuroscience* 7:615–630. [CrossRef Medline](#)
- Khairbek MA, Britt JP, Beeler JA, Ishikawa Y, McGehee DS, Zhuang X (2009) Adenylyl cyclase type 5 contributes to corticostriatal plasticity and striatum-dependent learning. *J Neurosci* 29:12115–12124. [CrossRef Medline](#)
- Kintscher M, Wozny C, Johnenning FW, Schmitz D, Breustedt J (2013) Role of RIM1alpha in short- and long-term synaptic plasticity at cerebellar parallel fibres. *Nat Commun* 4:2392. [CrossRef Medline](#)
- Kiyonaka S, Wakamori M, Miki T, Uriu Y, Nonaka M, Bito H, Beedle AM, Mori E, Hara Y, De Waard M, Kanagawa M, Itakura M, Takahashi M, Campbell KP, Mori Y (2007) RIM1 confers sustained activity and neurotransmitter vesicle anchoring to presynaptic Ca^{2+} channels. *Nat Neurosci* 10:691–701. [CrossRef Medline](#)
- Kreitzer AC, Malenka RC (2005) Dopamine modulation of state-dependent endocannabinoid release and long-term depression in the striatum. *J Neurosci* 25:10537–10545. [CrossRef Medline](#)
- Kupferschmidt DA, Lovinger DM (2015) Inhibition of presynaptic calcium transients in cortical inputs to the dorsolateral striatum by metabotropic GABA(B) and mGlu2/3 receptors. *J Physiol* 593:2295–2310. [CrossRef Medline](#)
- Kupferschmidt DA, Juczewski K, Cui G, Johnson KA, Lovinger DM (2017) Parallel, but dissociable, processing in discrete corticostriatal inputs encodes skill learning. *Neuron* 96:476–489.e5. [CrossRef Medline](#)
- Legault M, Wise RA (2001) Novelty-evoked elevations of nucleus accumbens dopamine: dependence on impulse flow from the ventral subiculum and glutamatergic neurotransmission in the ventral tegmental area. *Eur J Neurosci* 13:819–828. [CrossRef Medline](#)
- Lisman JE, Grace AA (2005) The hippocampal-VTA loop: controlling the entry of information into long-term memory. *Neuron* 46:703–713. [CrossRef Medline](#)
- Lonart G, Schoch S, Kaeser PS, Larkin CJ, Südhof TC, Linden DJ (2003) Phosphorylation of RIM1alpha by PKA triggers presynaptic long-term potentiation at cerebellar parallel fiber synapses. *Cell* 115:49–60. [CrossRef Medline](#)
- Lovinger DM (1991) Trans-1-aminocyclopentane-1,3-dicarboxylic acid (t-ACPD) decreases synaptic excitation in rat striatal slices through a presynaptic action. *Neurosci Lett* 129:17–21. [CrossRef Medline](#)
- Lovinger DM (2010) Neurotransmitter roles in synaptic modulation, plasticity and learning in the dorsal striatum. *Neuropharmacology* 58:951–961. [CrossRef Medline](#)
- Mathur BN, Capik NA, Alvarez VA, Lovinger DM (2011) Serotonin induces long-term depression at corticostriatal synapses. *J Neurosci* 31:7402–7411. [CrossRef Medline](#)
- McGeorge AJ, Faull RL (1989) The organization of the projection from the cerebral cortex to the striatum in the rat. *Neuroscience* 29:503–537. [CrossRef Medline](#)
- Miyachi S, Hikosaka O, Lu X (2002) Differential activation of monkey striatal neurons in the early and late stages of procedural learning. *Exp Brain Res* 146:122–126. [CrossRef Medline](#)
- Nazzaro C, Greco B, Cerovic M, Baxter P, Rubino T, Trusel M, Parolaro D, Tkatch T, Benfenati F, Pedarzani P, Tonini R (2012) SK channel modulation rescues striatal plasticity and control over habit in cannabinoid tolerance. *Nat Neurosci* 15:284–293. [CrossRef Medline](#)
- O'Hare JK, Li H, Kim N, Gaidis E, Ade K, Beck J, Yin H, Calakos N (2017) Striatal fast-spiking interneurons selectively modulate circuit output and are required for habitual behavior. *Elife* 6:26231. [CrossRef Medline](#)
- Park H, Popescu A, Poo MM (2014) Essential role of presynaptic NMDA receptors in activity-dependent BDNF secretion and corticostriatal LTP. *Neuron* 84:1009–1022. [CrossRef Medline](#)
- Peak J, Hart G, Balleine BW (2018) From learning to action: the integration of dorsal striatal input and output pathways in instrumental conditioning. *Eur J Neurosci*. Advance online publication. Retrieved May 23, 2018. doi: 10.1111/ejn.13964.
- Pittenger C, Fasano S, Mazzocchi-Jones D, Dunnett SB, Kandel ER, Brambilla R (2006) Impaired bidirectional synaptic plasticity and procedural memory formation in striatum-specific cAMP response element-binding protein-deficient mice. *J Neurosci* 26:2808–2813. [CrossRef Medline](#)
- Powell CM, Schoch S, Monteggia L, Barrot M, Matos MF, Feldmann N, Südhof TC, Nestler EJ (2004) The presynaptic active zone protein RIM1alpha is critical for normal learning and memory. *Neuron* 42:143–153. [CrossRef Medline](#)
- Richardson NR, Roberts DC (1996) Progressive ratio schedules in drug self-administration studies in rats: a method to evaluate reinforcing efficacy. *J Neurosci Methods* 66:1–11. [CrossRef Medline](#)
- Rueda-Orozco PE, Robbe D (2015) The striatum multiplexes contextual and kinematic information to constrain motor habits execution. *Nat Neurosci* 18:453–460. [CrossRef Medline](#)
- Russo SJ, Dietz DM, Dumitriu D, Morrison JH, Malenka RC, Nestler EJ (2010) The addicted synapse: mechanisms of synaptic and structural plasticity in nucleus accumbens. *Trends Neurosci* 33:267–276. [CrossRef Medline](#)
- Salamone JD, Correa M, Mingote S, Weber SM (2003) Nucleus accumbens

- dopamine and the regulation of effort in food-seeking behavior: implications for studies of natural motivation, psychiatry, and drug abuse. *J Pharmacol Exp Ther* 305:1–8. [CrossRef Medline](#)
- Salamone JD, Pardo M, Yohn SE, López-Cruz L, SanMiguel N, Correa M (2016) Mesolimbic dopamine and the regulation of motivated behavior. *Curr Top Behav Neurosci* 27:231–257. [CrossRef Medline](#)
- Santos FJ, Oliveira RF, Jin X, Costa RM (2015) Corticostriatal dynamics encode the refinement of specific behavioral variability during skill learning. *Elife* 4:e09423. [CrossRef Medline](#)
- Schmittgen TD, Livak KJ (2008) Analyzing real-time PCR data by the comparative C(T) method. *Nat Protoc* 3:1101–1108. [CrossRef Medline](#)
- Schoch S, Castillo PE, Jo T, Mukherjee K, Geppert M, Wang Y, Schmitz F, Malenka RC, Südhof TC (2002) RIM1alpha forms a protein scaffold for regulating neurotransmitter release at the active zone. *Nature* 415:321–326. [CrossRef Medline](#)
- Schoch S, Mittelstaedt T, Kaeser PS, Padgett D, Feldmann N, Chevaleyre V, Castillo PE, Hammer RE, Han W, Schmitz F, Lin W, Südhof TC (2006) Redundant functions of RIM1alpha and RIM2alpha in Ca(2+)-triggered neurotransmitter release. *EMBO J* 25:5852–5863. [CrossRef Medline](#)
- Shonesy BC, Wang X, Rose KL, Ramikie TS, Cavener VS, Rentz T, Baucum AJ 2nd, Jalan-Sakrikar N, Mackie K, Winder DG, Patel S, Colbran RJ (2013) CaMKII regulates diacylglycerol lipase-alpha and striatal endocannabinoid signaling. *Nat Neurosci* 16:456–463. [CrossRef Medline](#)
- Smith KS, Graybiel AM (2013) A dual operator view of habitual behavior reflecting cortical and striatal dynamics. *Neuron* 79:361–374. [CrossRef Medline](#)
- Smith Y, Raju DV, Pare JF, Sidibe M (2004) The thalamostriatal system: a highly specific network of the basal ganglia circuitry. *Trends Neurosci* 27:520–527. [CrossRef Medline](#)
- Südhof TC (2013) Neurotransmitter release: the last millisecond in the life of a synaptic vesicle. *Neuron* 80:675–690. [CrossRef Medline](#)
- Sun L, Bittner MA, Holz RW (2003) Rim, a component of the presynaptic active zone and modulator of exocytosis, binds 14–3-3 through its N terminus. *J Biol Chem* 278:38301–38309. [CrossRef Medline](#)
- Thomson AM (2000) Facilitation, augmentation and potentiation at central synapses. *Trends Neurosci* 23:305–312. [CrossRef Medline](#)
- Thorn CA, Atallah H, Howe M, Graybiel AM (2010) Differential dynamics of activity changes in dorsolateral and dorsomedial striatal loops during learning. *Neuron* 66:781–795. [CrossRef Medline](#)
- Wang Y, Okamoto M, Schmitz F, Hofmann K, Südhof TC (1997) Rim is a putative Rab3 effector in regulating synaptic-vesicle fusion. *Nature* 388:593–598. [CrossRef Medline](#)
- Wilson CJ (1995) The contribution of cortical neurons to the firing pattern of striatal spiny neurons. In *Models of information processing in the basal ganglia* (Houk JC, Davis JL, Beiser DG, eds), pp 29–50. Cambridge, MA: Massachusetts Institute of Technology.
- Wu YW, Kim JI, Tawfik VL, Lalchandani RR, Scherrer G, Ding JB (2015) Input- and cell-type-specific endocannabinoid-dependent LTD in the striatum. *Cell Rep* 10:75–87. [CrossRef Medline](#)
- Yang Y, Calakos N (2010) Acute in vivo genetic rescue demonstrates that phosphorylation of RIM1alpha serine 413 is not required for mossy fiber long-term potentiation. *J Neurosci* 30:2542–2546. [CrossRef Medline](#)
- Yin HH, Knowlton BJ, Balleine BW (2004) Lesions of dorsolateral striatum preserve outcome expectancy but disrupt habit formation in instrumental learning. *Eur J Neurosci* 19:181–189. [CrossRef Medline](#)
- Yin HH, Knowlton BJ, Balleine BW (2005a) Blockade of NMDA receptors in the dorsomedial striatum prevents action-outcome learning in instrumental conditioning. *Eur J Neurosci* 22:505–512. [CrossRef Medline](#)
- Yin HH, Ostlund SB, Knowlton BJ, Balleine BW (2005b) The role of the dorsomedial striatum in instrumental conditioning. *Eur J Neurosci* 22:513–523. [CrossRef Medline](#)
- Yin HH, Knowlton BJ, Balleine BW (2006) Inactivation of dorsolateral striatum enhances sensitivity to changes in the action-outcome contingency in instrumental conditioning. *Behav Brain Res* 166:189–196. [CrossRef Medline](#)
- Yin HH, Mulcare SP, Hilário MR, Clouse E, Holloway T, Davis MI, Hansson AC, Lovinger DM, Costa RM (2009) Dynamic reorganization of striatal circuits during the acquisition and consolidation of a skill. *Nat Neurosci* 12:333–341. [CrossRef Medline](#)